



Dynamic seasonal nitrogen cycling in response to anthropogenic N loading in a tropical catchment, Athi–Galana–Sabaki River, Kenya

T. R. Marwick¹, F. Tamooch^{1,2}, B. Ogwoka², C. Teodoru¹, A. V. Borges³, F. Darchambeau³, and S. Bouillon¹

¹Katholieke Universiteit Leuven (KU Leuven), Department of Earth and Environmental Sciences, Celestijnenlaan 200E, 3001 Leuven, Belgium

²Kenya Wildlife Service, P.O. Box 82144-80100, Mombasa, Kenya

³Unité d’Océanographie Chimique, Université de Liège (ULg), Liège, Belgium

Correspondence to: T. R. Marwick (trenrichard.marwick@ees.kuleuven.be)

Received: 19 April 2013 – Published in Biogeosciences Discuss.: 23 May 2013

Revised: 3 October 2013 – Accepted: 11 December 2013 – Published: 29 January 2014

Abstract. As part of a broader study on the riverine biogeochemistry in the Athi–Galana–Sabaki (A-G-S) River catchment (Kenya), we present data constraining the sources, transit and transformation of multiple nitrogen (N) species as they flow through the A-G-S catchment ($\sim 47\,000\text{ km}^2$). The data set was obtained in August–September 2011, November 2011, and April–May 2012, covering the dry season, short rain season and long rain season respectively. Release of (largely untreated) wastewater from the city of Nairobi had a profound impact on the biogeochemistry of the upper Athi River, leading to low dissolved oxygen (DO) saturation levels (36–67%), high ammonium (NH_4^+) concentrations ($123\text{--}1193\ \mu\text{mol L}^{-1}$), and high dissolved methane (CH_4) concentrations ($3765\text{--}6729\ \text{nmol L}^{-1}$). Riverine dissolved inorganic nitrogen (DIN; sum of NH_4^+ and nitrate (NO_3^-); nitrite was not measured) concentration at the most upstream site on the Athi River was highest during the dry season ($1195\ \mu\text{mol L}^{-1}$), while DIN concentration was an order of magnitude lower during the short and long rain seasons (212 and $193\ \mu\text{mol L}^{-1}$ respectively). During the rain seasons, low water residence time led to relatively minimal in-stream N cycling prior to discharge to the ocean, whereas during the dry season we speculate that prolonged residence time creates two differences comparative to wet season, where (1) intense N cycling and removal of DIN is possible in the upper to mid-catchment and leads to significantly lower concentrations at the outlet during the dry season, and (2) as a result this leads to the progressive enrichment of ^{15}N in the particulate N (PN) pool, highlighting the dominance of untreated wastewater as the prevailing source of riverine DIN.

The rapid removal of NH_4^+ in the upper reaches during the dry season was accompanied by a quantitatively similar production of NO_3^- and nitrous oxide (N_2O) downstream, pointing towards strong nitrification over this reach during the dry season. Nitrous oxide produced was rapidly degassed downstream, while the elevated NO_3^- concentrations steadily decreased to levels observed elsewhere in more pristine African river networks. Low pelagic primary production rates over the same reach suggest that benthic denitrification was the dominant process controlling the removal of NO_3^- , although large cyanobacterial blooms further downstream highlight the significant role of DIN assimilation by primary producers also. Consequently, the intense nitrification and uptake of N by algae leads to significant enrichment of ^{15}N in the PN pool during the dry season (mean: $+16.5 \pm 8.2\text{‰}$ but reaching as high as $+31.5\text{‰}$) compared to the short ($+7.3 \pm 2.6\text{‰}$) and long ($+7.6 \pm 5.9\text{‰}$) rain seasons. A strong correlation between the seasonal N stable isotope ratios of PN ($\delta^{15}\text{N}_{\text{PN}}$) and oxygen stable isotope ratios of river water ($\delta^{18}\text{O}_{\text{H}_2\text{O}}$; as a proxy of freshwater discharge) presents the possibility of employing a combination of proxies – such as $\delta^{15}\text{N}_{\text{PN}}$ of sediments, bivalves and near-shore corals – to reconstruct how historical land use changes have influenced nitrogen cycling within the catchment, whilst potentially providing foresight on the impacts of future land management decisions.

1 Introduction

Human activities over the last two centuries have drastically influenced regional and global nitrogen (N) cycles (Galloway et al., 1995; Howarth et al., 1996; Galloway and Cowling, 2002). Prior to the Industrial Revolution, the dominant processes fixing atmospheric dinitrogen (N_2) to reactive (biologically available) N were lightning, bacterial nitrogen fixation (BNF) and volcanic activity, while the return of N_2 gases to the atmosphere through the denitrification and anammox pathways closed the global N cycle (Ayres et al., 1994; Canfield et al., 2010). Post-Industrial Revolution, and linked with the demands of an expanding global population, the development of the Haber–Bosch process (and increasing synthetic fertiliser application), fossil fuel combustion, and the increased cultivation of BNF crops now account for about 45 % of total annual fixed N produced globally (Canfield et al., 2010). Within agro-ecosystems, for example, of the approximately 170 Tg N yr^{-1} introduced to crops globally, over 70 % of this N may be lost to the atmosphere and regional waters annually (Galloway et al., 2003). Upon entering river systems through point source (predominantly urban and industrial effluents) or diffusive source (such as leaching from agricultural land and atmospheric deposition) pathways (Bouwman et al., 2005), insufficient storage or removal of N may lead to severe environmental consequences downstream, including eutrophication, acidification of water bodies, fish kills, loss of biodiversity (Vitousek et al., 1997; Carpenter et al., 1998), as well as the rising emission of nitrous oxide (N_2O) to the atmosphere (Seitzinger and Kroeze, 1998), a potent greenhouse gas (with a global warming potential ~ 300 times greater than carbon dioxide) and the leading ozone-depleting substance in the 21st century (Ravishankara et al., 2009).

The dominant forms of reactive N (i.e. dissolved inorganic nitrogen, DIN) entering freshwaters are ammonium (NH_4^+) and nitrate (NO_3^-), albeit in low concentrations unless inputs are linked to N-saturated forests, grasslands, agroecosystems, or suburban landscapes (Galloway et al., 2003). A network of microbial metabolic pathways and abiotic reactions are involved in the transformation and removal of N from aquatic systems, including N_2 fixation, ammonification, anaerobic NH_4^+ oxidation (anammox), nitrification, denitrification, dissimilatory reduction of NO_3^- to NH_4^+ (DNRA), assimilation of DIN into biomass, NH_3 volatilization, and NH_4^+ adsorption and desorption. These pathways may be (chemo)autotrophic or heterotrophic, with the prevailing pathway dependant on the presence or absence of oxygen and organic carbon (OC) within the local environment (Trimmer et al., 2012). Resource stoichiometry (OC : NO_3^-) may also control NO_3^- accumulation and transformation within a system through the regulation of various microbial processes linking the nitrogen and carbon cycles (Taylor and Townsend, 2010). Water residence time and the

NO_3^- load per unit area of sediment are also important in constraining the quantity of DIN removed at the reach scale. Under high-flow conditions (and/or high N loading) there may be comparatively minimal turnover of total NO_3^- load at the reach scale (Trimmer et al., 2012), whereas prolonged water residence time provides greater opportunity for contact between DIN in the water column and (oxic) surface and (anoxic) hyporheic sediments.

Despite the low residence time of fluvial transported materials within the aquatic system relative to their terrestrial residence times, rivers can efficiently remove DIN, often denitrifying as much as 30 to 70 % of external N inputs (Galloway et al., 2003). Lakes and reservoirs are two features which prolong residence time within a river network by enhancing particle settling and nutrient processing, through which N removal may proceed by sedimentation and/or through N-removal processes (Wetzel, 2001). Recent modelling of these lentic systems conservatively estimates their ability to remove $19.7 \text{ Tg N yr}^{-1}$ globally (Harrison et al., 2009), with small lakes ($< 50 \text{ km}^2$) accounting for 9.3 Tg N yr^{-1} , while reservoirs (making up only 6 % of the global lentic surface area) are estimated to retain 33 % of N removed globally by lentic systems. Clearly, upstream lakes and reservoirs have a significant ability to remove N from river systems, and can effectively alleviate the downstream consequences listed previously.

Within the oxygenated zone of the water column, chemoautotrophic bacteria (e.g. *Nitrosomonas* sp., *Nitrosococcus* sp.) and archaea (*Nitrosopumilus*, *Nitrosotalea*, *Nitrosocaldus*; Cao et al., 2013) oxidise NH_4^+ to nitrite (NO_2^-), with the NO_2^- subsequently oxidised to NO_3^- by an alternate group of bacteria (*Nitrobacter* sp.), completing the nitrification pathway. The relative importance of archaea and bacteria in NH_4^+ oxidation and the related environmental drivers are still poorly constrained, particularly in freshwater environments (French et al., 2012; Hugoni et al., 2013). Removal of NO_3^- by fluvial systems may occur through denitrification, via the production and efflux of N_2 and N_2O gas to the atmosphere. The production of N_2O is avoided through the anammox pathway, a two-step process by which NH_4^+ is initially converted to the intermediate N_2H_4 and finally N_2 gas (Canfield et al., 2010). Denitrification, another anaerobic pathway operating in anoxic zones, reduces the NO_3^- produced during nitrification to either N_2O or N_2 gases. N_2O can also be produced as a by-product during nitrification, although denitrification is assumed to be the dominant process producing N_2O in temperate freshwaters (Beaulieu et al., 2011). Ammonia oxidisers can also produce N_2O through nitrifier denitrification (Wrage et al., 2001).

The use of nitrogen stable isotope ratios ($\delta^{15}N$) is a valuable tool to delineate the sources of N in aquatic systems (Risk et al., 2009). This approach is based on the preferential involvement of the isotopically lighter ^{14}N , relative to the heavier ^{15}N , in various biogeochemical reactions, resulting

in isotopic fractionation of the residual N pool and the pool of the product (Owens, 1987). The dominant sources of N to aquatic systems often have distinguishable $\delta^{15}\text{N}$ signatures. Biological fixation of atmospheric N ($\delta^{15}\text{N} = 0\text{‰}$) generally results in minimal N isotope fractionation (0‰ to +2‰), while the production of artificial fertilizer produces $\delta^{15}\text{N}$ from -2‰ to $+4\text{‰}$ (Vitoria et al., 2004). Ammonium released with raw wastewater discharge may be characterised by $\delta^{15}\text{N}_{\text{NH}_4^+}$ values between 7‰ and 12‰ (Sebilo et al., 2006), while, following nitrification, nitrate typically displays $\delta^{15}\text{N}_{\text{NO}_3^-}$ of $+8\text{‰}$ to $+22\text{‰}$ (Aravena et al., 1993; Widory et al., 2005). Recent studies have employed this technique to trace the movement of sewage-derived N within aquatic ecosystems (e.g. Costanzo et al., 2001; De Brabandere et al., 2002; Lapointe et al., 2005; Risk et al., 2009; Moynihan et al., 2012). For example, Elliot and Brush (2006) correlated a $+2\text{‰}$ to $+7\text{‰}$ change in $\delta^{15}\text{N}$ of a wetland sedimented organic matter core spanning 350 yr to a shift in land use from forested conditions to increased nutrient inputs from human waste, highlighting the potential of this technique to expand our temporal frame for assessing land use change on catchment N cycling.

To date, increased DIN inputs have had most severe environmental impact in developed countries of the temperate zone, largely driven by synthetic fertiliser application (Holland et al., 1999; Howarth, 2008). Yet, rapidly increasing populations in developing countries of the tropics are leading to increased ecosystem N loading within these regions also, with the consequences already being observed and forecasted (Caraco and Cole, 1999; Downing et al., 1999; Bowman et al., 2005; Seitzinger et al., 2010). Models suggest that coastal waters of African river catchments have experienced a 35% increase in DIN yield from 1970 to 2000, with two thirds of this entering the oceans within the 0–35 S latitude band (Yasin et al., 2010). A further 4–47% increase in total river export of DIN is modelled for the period 2000–2050, with the quantity of anthropogenically influenced N fixation exceeding natural (pre-industrial) N_2 fixation rates.

Through draining the city of Nairobi, Kenya, the Athi–Galana–Sabaki (A-G-S) catchment provides an example of the consequences of N loading within inland water systems of tropical Africa. Following British settlement and the establishment of Nairobi in 1899, the urban population swelled from 11 500 in 1906 (Olima, 2001) to over 3.1 million by 2009 (K.N.B.S., 2009). Approximately half the current population of Nairobi live in slums lacking adequate sewage and sanitation services (Dafe, 2009). Numerous informal settlements are located within the riparian fringe of the Athi River headwaters (Kithiia, 2012). Poor waste disposal and management strategies have led to increasing water quality degradation (Kithiia and Wambua, 2010), where, for example, the total quantity of water passing through the A-G-S headwater streams ($36.7 \times 10^6 \text{ m}^3 \text{ yr}^{-1}$) and into the main channel equates to less than the combined domestic and industrial waste discharge for the region (Kithiia, 2012).

Previous research has revealed substantial changes in the A-G-S catchment over the past decennia. Based on geochemical data recorded in corals near the Sabaki River mouth, Fleitmann et al. (2007) suggested a stable riverine sediment flux at the outlet between 1700 and 1900, but a 5- to 10-fold increase in sediment delivery up to the period 1974–1980. The increase has been attributed to the expansion of intensive agricultural practises in the headwaters, unregulated land use, deforestation, and severe droughts in the 1970s. Yet, little is known of the temporal and spatial processes controlling the transport and cycling of N through the A-G-S network.

As part of a broader study on the riverine biogeochemistry in the A-G-S catchment, we present data collected during three climatic seasons and a one-year bi-weekly sampling regime to constrain the sources, transformations and transit of multiple N species as they pass through the A-G-S River, stretching from downstream of urban Nairobi to the outlet at the Indian Ocean.

2 Materials and methods

2.1 Study area

The Athi–Galana–Sabaki catchment, the second-largest river network in Kenya, drains a total catchment area of 46 600 km². The headwaters of the A-G-S catchment are situated in central and south-east Kenya, in the vicinity of Nairobi city (Fig. 1). Upstream of Nairobi, the headwaters forming the Nairobi River drain agricultural areas (predominantly tea and coffee plantations) which provide the livelihood of 70% of the regional population (Kithiia, 1997). Industrial activities and informal settlements dominate the sub-catchment around Nairobi, with livestock and small-scale irrigation activities also present downstream, prior to the confluence of the Nairobi River with the Athi River at 1440 m above sea level (m a.s.l.) and 590 km from the Indian Ocean. Climatic variability and post-settlement land uses within the region have resulted in severe soil erosion and increased sediment transport from headwater catchments (Kithiia, 1997; Kithiia et al., 2004; Fleitmann et al., 2007). Downstream of the Athi–Nairobi confluence, the river follows a confined channel along the southern edge of the Yatta Plateau between Thika and Voi before receiving the Tsavo River (at 240 m a.s.l.), the only major perennial tributary other than the Nairobi River, which drains the northern slopes of Mount Kilimanjaro. Ephemeral tributaries emanate from Amboseli, Chyulu Hills and Taita Hills in the mid-catchment. Again, severe soil erosion in the mid-catchment, particularly within the agricultural Machakos district, dates back to the 1930s (Tiffen et al., 1994), and has been linked to the felling of vegetation for charcoal burning, poor cultivation methods and over-grazing (Ongwenyi et al., 1993). Downstream of the Athi–Tsavo confluence the river takes the name Galana, opening out into a broad floodplain with a meandering habit

(Oosterom, 1988). The Galana River follows this habit for 220 km through semi-arid savannah plains before emptying into the west Indian Ocean near the Malindi–Watamu reef complex as the Sabaki River. Seawater incursion is impeded in the lower reaches of the Sabaki as a result of a relatively steep gradient ($3 \times 10^{-4} \text{ mm}^{-1}$).

Annual precipitation ranges between 800 and 1200 mm yr^{-1} in the highly populated central highlands (Fig. 2), to 400–800 mm yr^{-1} in the less populated semi-arid south-east. Annually, two dry seasons are interspersed by a long (March–May, MAM) and short (October–December, OND) rain season. Accordingly, the hydrograph displays bimodal discharge, with seasonal variation measured between $0.5 \text{ m}^3 \text{ s}^{-1}$ and $758 \text{ m}^3 \text{ s}^{-1}$ (1957–1979 mean: $48.8 \text{ m}^3 \text{ s}^{-1}$) (Fleitmann et al., 2007). No continuous discharge measurements were available for our sampling period, yet we believe the in situ conditions observed across sampling campaigns were representative of the seasonality and hydrograph in Fig. 2. Recent data (2001–2004) place mean discharge at $73.0 \text{ m}^3 \text{ s}^{-1}$ at the outlet (Kitheka et al., 2004). Mean annual flow of the perennial Tsavo River has increased from $4 \text{ m}^3 \text{ s}^{-1}$ to $10 \text{ m}^3 \text{ s}^{-1}$ between the 1950s and present conditions, attributed to increased melting of glaciers on Mount Kilimanjaro (Kitheka et al., 2004). Oscillations between El Niño and La Niña conditions in Kenya have a strong influence on the decadal patterns of river discharge, where extended severe drought can be broken by intense and destructive flooding (Mogaka et al., 2006). No reservoirs have yet been developed within the catchment for the harnessing of hydropower (Kitheka et al., 2004), although a number of small abandoned dams, originally for industrial water abstraction purposes, are present in the Nairobi headwaters (e.g. Nairobi Dam). The combination of changing land use practices, highly variable climatic conditions and highly erosive native soils has led to modern sediment flux estimates between 7.5 and 14.3 million t yr^{-1} (Van Katwijk et al., 1993), equating to a soil erosion rate of 110–210 $\text{t km}^{-2} \text{ yr}^{-1}$.

2.2 Sampling and analytical techniques

Sampling was conducted at 20–25 sites throughout the A-G-S catchment at the end of the long dry season (August–September 2011), and during the short rain (November 2011) and long rain seasons (April 2012). The primary focus of the research was riverine carbon cycling in tropical catchments, and we did not sample for the N isotopes of DIN in the study. Similarly, headwater regions above and within Nairobi were ignored due to the overriding influence of pollutants on stream quality. Fourteen Falls, 23 km downstream of the Athi–Nairobi confluence, was selected as the most upstream sampling site, with another 14 sites downstream at approximately 40 km intervals leading to the outlet. The most downstream site, S20 (5 km upstream of the river mouth), was equipped to sample fortnightly, commencing August 2011.

The sole sub-catchment sampled during the dry season was the Tsavo (5 sites replicated), whereas during both the OND and MAM rains it was possible to sample within the Keite (4 and 3 sites sampled during the OND and MAM rain seasons respectively) and Muoni (1 site sampled during both rain seasons) catchments also.

In situ physico-chemical parameters, including water temperature, dissolved oxygen (DO) content, and pH, were measured using a combination of a YSI Professional Plus (Pro Plus, Quatro Cable bulkhead) and YSI Professional Optical Dissolved Oxygen (ProODO) instrument. Calibrations for pH were performed daily using National Bureau of Standards (NBS) buffers of pH 4 and 7.

Water samples for nutrient analysis (NH_4^+ and NO_3^-) were obtained in 20 mL scintillation vials by pre-filtering surface water through pre-combusted GF/F filters ($0.7 \mu\text{m}$), with further filtration through $0.2 \mu\text{m}$ syringe filters and preserved with 20 μL of saturated HgCl_2 . Nitrite was not measured, and hence total DIN refers to the sum of NH_4^+ and NO_3^- . Samples for analysis of $\delta^{15}\text{N}_{\text{PN}}$ were obtained by filtering a known volume of surface water on pre-combusted (overnight at 450°C) 47 mm GF/F filters ($0.7 \mu\text{m}$). Filters were dried and a section from each filter packed into Ag cups for $\delta^{15}\text{N}_{\text{PN}}$ analysis. Samples for particulate organic carbon (POC), particulate N (PN), and $\delta^{13}\text{C}_{\text{POC}}$ were obtained in the same manner as $\delta^{15}\text{N}_{\text{PN}}$ samples, though filtered through a pre-combusted (500°C for 4 h) 25 mm GF/F filter (nominal porosity = $0.7 \mu\text{m}$) which was air-dried on site. These filters were later exposed to HCl fumes for 4 h to remove inorganic C, re-dried and packed in Ag cups.

A Niskin bottle was used to collect surface water for dissolved methane (CH_4) and N_2O samples. Samples were stored in 60 mL glass serum vials, preserved with the addition of 20 μL HgCl_2 , closed air-tight with a butyl stopper, and sealed with an aluminium cap. Remaining water from the Niskin bottle was used for measuring community respiration rates. Between 5 and 7 borosilicate biological oxygen demand bottles with stoppers (60 mL volume; Wheaton) were over-filled, sealed and stored in an isothermal insulated box. After approximately 24 h, DO (mg L^{-1}) was measured and used to calculate an average community respiration rate (R):

$$R = \frac{\text{DO}_r - \text{DO}_i}{t_e - t_i}, \quad (1)$$

where DO_r is the in situ DO (mg L^{-1}) of the river water, DO_i the DO (mg L^{-1}) following incubation, and t_i and t_e the initial and end time of the incubation. During the dry season campaign, DO_r was assumed from the in-stream measurements of the YSI ProODO instrument, whereas during the OND and MAM rain campaigns three extra incubation bottles were filled and the DO (mg L^{-1}) immediately measured using the YSI ProODO instrument, with the average of the three bottles used as DO_r .

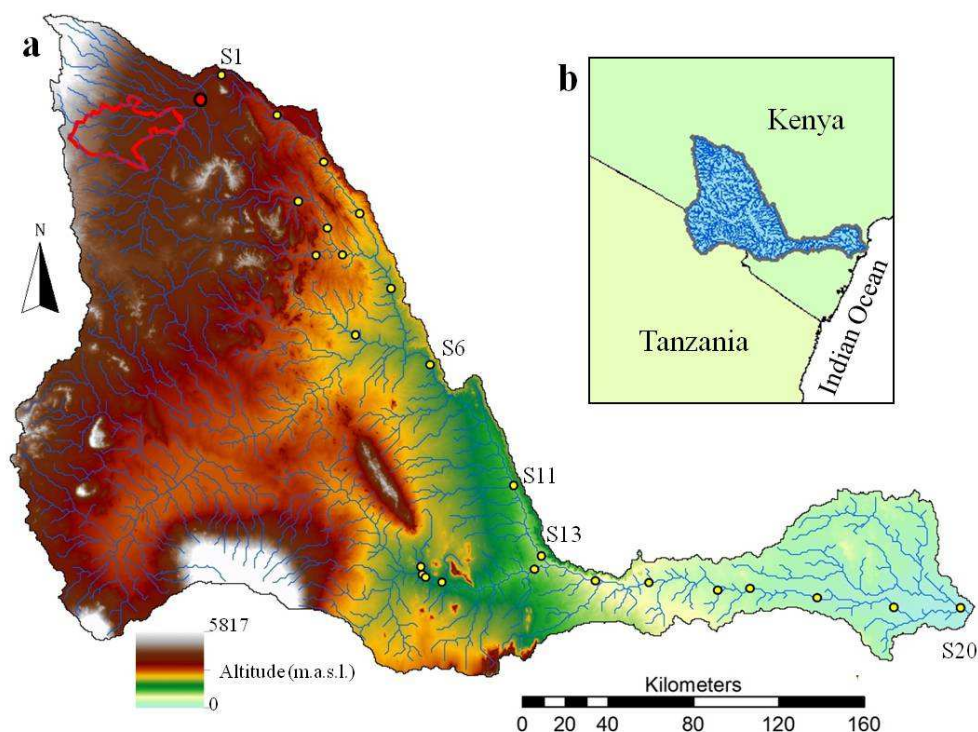


Fig. 1. (a) Digital elevation model (DEM) of Athi–Galana–Sabaki (A–G–S) River catchment (yellow circles = sample sites). The Nairobi River drains the area upstream of and within the Nairobi city administration boundary (red polygon), with the red circle indicating the confluence with the Athi River. Downstream of S13 the Athi River is joined on its right bank by the Tsavo, draining the areas below Mount Kilimanjaro in the south-west of the catchment. Downstream of the Athi–Tsavo confluence, the river takes the name Galana. The river is referred to as the Sabaki River in the vicinity of S20. (b) The inset map shows the position of the A–G–S catchment within south-eastern Kenya and north-eastern Tanzania.

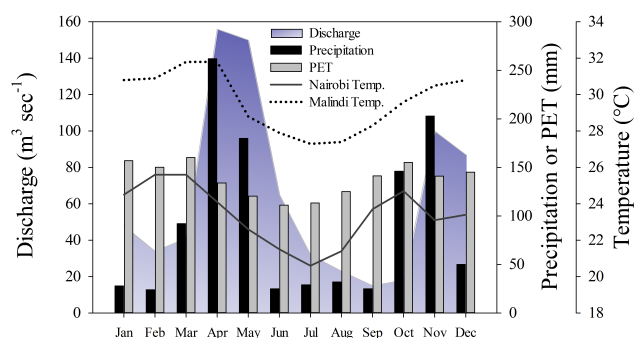


Fig. 2. Mean monthly variation of hydrological and climate parameters in the Athi–Galana–Sabaki catchment, including discharge at the outlet (shaded area; data from 1959–1977), precipitation (black bar) (from Fleitmann et al., 2007), potential evapotranspiration (PET; grey box), and the maximum air temperature in Nairobi (A–G–S headwaters; solid grey line) and Malindi (A–G–S outlet; dotted black line).

Water samples for total alkalinity (TA) were obtained by pre-filtering surface water through pre-combusted GF/F filters (0.7 μm), with further filtration through 0.2 μm syringe

filters in high-density polyethylene bottles. TA was analysed by automated electro-titration on 50 mL samples with 0.1 mol L⁻¹ HCl as titrant (reproducibility estimated as better than $\pm 3 \mu\text{mol kg}^{-1}$ based on replicate analyses).

In situ pelagic primary production measurements were performed by filling two 500 mL polycarbonate bottles with surface water and adding 500 μL of a ¹³C-spike solution (> 99.8 % ¹³C NaH¹³CO₃, $\pm 40 \text{ mg}$ dissolved in 12 mL of 0.2 μm filtered surface water). Bottles were incubated in-stream under ambient light and temperature conditions for approximately 2 h, after which a subsample from each bottle was filtered onto separate pre-combusted (500 °C for 4 h) 25 mm GF/F filter (nominal porosity = 0.7 μm) and air-dried on site. These filters were later exposed to HCl fumes for 4 h to remove inorganic C, re-dried and packed in Ag cups. A separate 12 mL glass headspace vial, for measurement of the ¹³C-DIC enrichment ($\delta^{13}\text{C}_{\text{DIC-PP}}$), was also filled from each bottle with the addition of 10 μL HgCl₂ to inhibit further biological activity.

Analysis of primary production filters and the $\delta^{13}\text{C}_{\text{DIC-PP}}$ followed the procedures outlined below for POC and $\delta^{13}\text{C}_{\text{DIC}}$ respectively. Primary production rates (PP) were

calculated based on Hama et al. (1983):

$$PP = \frac{POC_f (\%^{13}POC_f - \%^{13}POC_i)}{t (\%^{13}DIC - \%^{13}POC_i)}, \quad (2)$$

where t is the incubation time, $\%^{13}DIC$ the percentage ^{13}C of the DIC after the bottles had been spiked, POC_f the particulate organic carbon after incubation, and $\%^{13}POC_i$ and $\%^{13}POC_f$ the initial and final (i.e. after incubation) percentage ^{13}C of the POC respectively. Where the difference between $\%^{13}POC_i$ and $\%^{13}POC_f$ was $< 1\%$, PP was considered below detection limits ($< d.l.$) at these sites.

Laboratory analysis of riverine NH_4^+ (based on the modified Berthelot reaction) and NO_3^- (based on the hydrazinium sulfate reduction method) concentration was conducted on a 5 mL subsample of the field sample, and measured on a Skalar Continuous Flow Analyzer (model 5100) with FlowAccess V3 software.

POC, PN, $\delta^{13}C_{POC}$ and $\delta^{15}N_{PN}$ were determined on a Thermo elemental analyser–isotope ratio mass spectrometer (EA-IRMS) system (FlashHT with DeltaV Advantage), using the thermal conductivity detector (TCD) signal of the EA to quantify PN, and by monitoring either the m/z 28 and 29 or m/z 44, 45, and 46 signal on the IRMS. Calibration of $\delta^{15}N_{PN}$ was performed with IAEA-N1, while IAEA-C6 and acetanilide were used for $\delta^{13}C_{POC}$, with all standards internally calibrated against international standards. Reproducibility of $\delta^{15}N_{PN}$ and $\delta^{13}C_{POC}$ measurements was typically better than $\pm 0.2\%$, while relative standard deviations for calibration standards for POC and PN measurements were typically $< 2\%$ and always $< 5\%$. POC:PN ratios are presented on a weight:weight basis. Throughout the text, $\%POC$ and $\%PN$ refer to the percentual contribution of POC and PN to the total suspended matter load (TSM).

Concentrations of CH_4 and N_2O were determined by a headspace equilibration technique (20 mL N_2 headspace in 60 mL serum bottles). Samples were shaken vigorously after creating the headspace, equilibrated overnight (min. 12 h) in a thermostated bath (constant temperature within $0.5^\circ C$ of the average of all in situ riverine water column temperature data), and again vigorously shaken prior to injection. Headspace gases were measured by gas chromatography (GC; Weiss, 1981) with flame ionization detection (FID) and electron capture detection (ECD). The SRI 8610C GC-FID-ECD was calibrated with $CH_4 : CO_2 : N_2O : N_2$ mixtures (Air Liquide Belgium) of 1, 10 and 30 ppm CH_4 and of 0.2, 2.0 and 6.0 ppm N_2O , and using the solubility coefficients of Yamamoto et al. (1976) for CH_4 and Weiss and Price (1980) for N_2O . For the calculation of CH_4 and N_2O saturation levels, atmospheric CH_4 mixing ratios were assumed constant (1.8 ppm), and monthly average measurements at Mauna Loa of N_2O atmospheric measurements were taken from the Chromatograph for Atmospheric Trace Species in situ Halocarbons Program database of the National Oceanic and Atmospheric Administration, Earth System Research Labora-

tory, Global Monitoring Division. Gas solubility of CH_4 and N_2O was computed according to Yamamoto et al. (1976) and Weiss and Price (1980) respectively.

$\delta^{18}O_{H_2O}$ analyses were conducted as described by Gillikin and Bouillon (2007). One half (0.5) mL of sampled water (from the bulk 20 mL nutrient sample) was added to a 12 mL glass headspace vial and subsequently flushed with He, followed by the addition of 0.25 mL of pure CO_2 gas using a gas-tight syringe. Following overnight equilibration, approximately 1 mL of the headspace was injected into the above-mentioned EA-IRMS configuration. Three internal working standards covering a range of $\delta^{18}O$ values between -22.3 and $+6.9\%$, calibrated versus SMOW (Vienna Standard Mean Ocean Water; 0%), GISP (Greenland Ice Sheet precipitation; -24.76%) and SLAP (Standard Light Antarctic precipitation; -55.50%) were used to calibrate sample $\delta^{18}O_{H_2O}$ data.

3 Results

Water temperature along the main channel increased downstream during all campaigns (Fig. 3a). DO saturation levels ranged 36.1–154.2%, 56.0–108.1% and 66.8–111.0% during the dry season, OND and MAM rains respectively, with surface waters nearing hypoxic conditions (DO saturation level $< 30\%$) at S1 (36.1% DO) and S2 (37.2%) during the dry season (Fig. 3b). DO was significantly higher (paired t test (PTT), $p = 0.07$, $n = 20$) during the dry season than during the OND rains, which were also significantly lower (PTT, $p = 0.05$, $n = 23$) than the MAM rains. In situ pH was significantly higher during the dry season (range: 7.2–9.8; mean: 8.4 ± 2.3) compared to both the OND (range: 7.2–8.6; mean: 7.3 ± 0.9) (PTT, $p = < 0.001$, $n = 20$) and MAM (range: 6.5–8.3; mean: 7.5 ± 0.5) (PTT, $p = < 0.001$, $n = 19$) rain seasons, particularly in the lower reaches of the main channel (Fig. 3c), while pH was also significantly lower (PTT, $p = 0.01$, $n = 23$) during the MAM rains comparative to OND rains.

Total DIN concentrations at S1 were highest during the dry season ($1195 \mu mol L^{-1}$), and almost completely in the form of NH_4^+ (99.8%). Total DIN was considerably lower at S1 during the OND ($430 \mu mol L^{-1}$) and MAM ($222 \mu mol L^{-1}$) rains, with NH_4^+ still the dominant DIN form entering the study area (72.0% and 55.4% respectively). Total DIN in the Tsavo River at S12 (9 km upstream from the Tsavo–Athi confluence, the single perennial tributary measured within the study area) displayed less variability (dry season: $56.5 \mu mol L^{-1}$; OND: $56.4 \mu mol L^{-1}$; MAM: $88.3 \mu mol L^{-1}$), and was dominated by NO_3^- across all seasons (dry season: 66.8% of total DIN; OND: 97.0%; MAM: 62.6%).

NH_4^+ decreased one to two orders of magnitudes from S1 to the outlet over all seasons (Fig. 4a). Concentrations ranged 13.8 – $1192.9 \mu mol L^{-1}$ (mean: $84.3 \pm 263.5 \mu mol L^{-1}$),

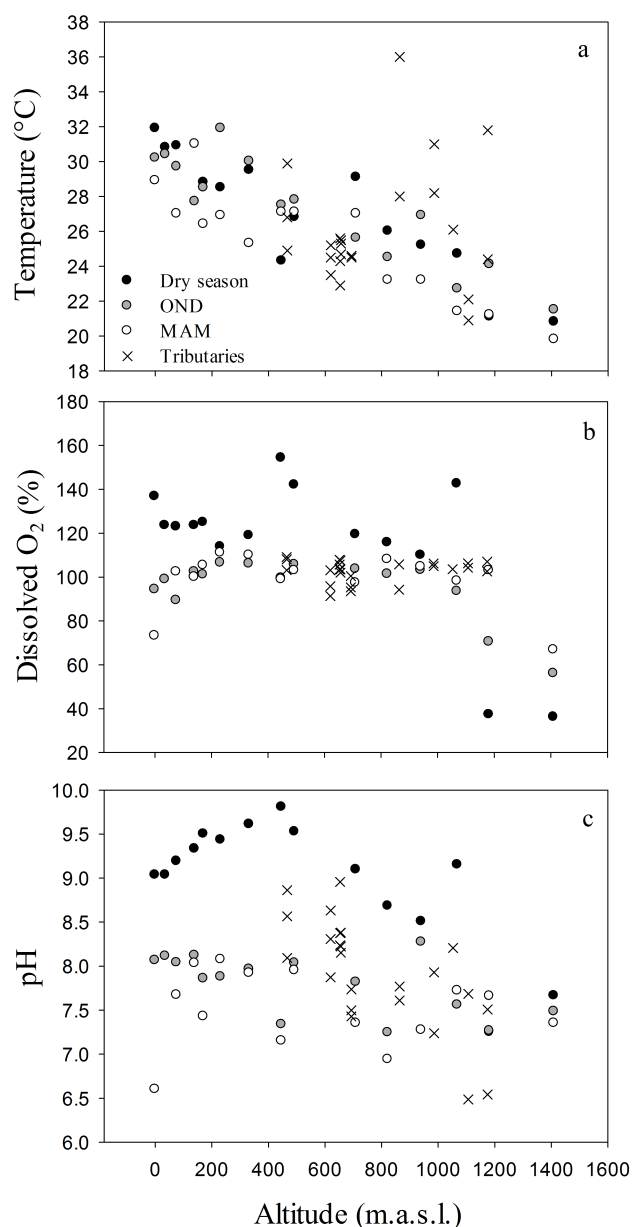


Fig. 3. Altitudinal gradient during dry season (August–September 2011), short rain season (October–December, OND, November 2011) and long rain season (March–May, MAM, April 2012) and tributaries (x, all seasons) of in-stream (a) temperature (°C), (b) dissolved oxygen (%), and (c) pH.

0.4–309.7 $\mu\text{mol L}^{-1}$ ($18.5 \pm 61.2 \mu\text{mol L}^{-1}$), and 8.4–123.0 $\mu\text{mol L}^{-1}$ ($24.2 \pm 25.7 \mu\text{mol L}^{-1}$) during the dry, OND and MAM rain season respectively. NH_4^+ concentrations during the OND rains were significantly higher than during the dry season (Wilcoxon signed rank test (WSRT), $p < 0.001$, $n = 20$) and MAM rains (WSRT, $p = 0.004$, $n = 22$). NO_3^- concentrations ranged 0.2–857.6 $\mu\text{mol L}^{-1}$ (dry season mean: $195.7 \pm 309.4 \mu\text{mol L}^{-1}$), 40.3–537.6 $\mu\text{mol L}^{-1}$ (OND rain mean: $188.5 \pm 145.4 \mu\text{mol L}^{-1}$), and 24.0–

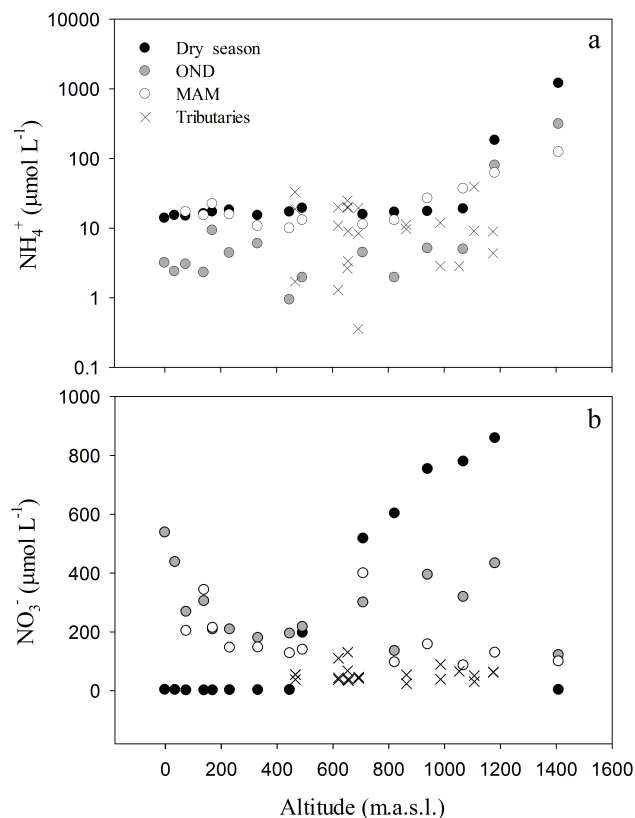


Fig. 4. Altitudinal gradient during dry season (August–September 2011), short rain season (October–December, OND, November 2011) and long rain season (March–May, MAM, April 2012) and tributaries (x, all seasons) of in-stream (a) NH_4^+ ($\mu\text{mol L}^{-1}$), and (b) NO_3^- ($\mu\text{mol L}^{-1}$). Note the logarithmic scale on the top panel.

398.8 $\mu\text{mol L}^{-1}$ (MAM rain mean: $127.7 \pm 95.5 \mu\text{mol L}^{-1}$) (Fig. 4b). When sites are split above and below 450 m a.s.l., NO_3^- concentrations < 450 m a.s.l. in the dry season are significantly lower than during both the OND (PTT, $p < 0.001$, $n = 8$) and MAM rains (PTT, $p = 0.002$, $n = 6$). The rapid decrease of NH_4^+ between S1 and S2 is accompanied by an increase of NO_3^- over the same stretch during all seasons, though being most pronounced in the dry season.

Like NO_3^- , dissolved N_2O peaked at S2 (196 nmol L^{-1}) during the dry season, decreasing rapidly by S3 (18 nmol L^{-1}) (Fig. 5a). Dissolved N_2O generally decreased downstream over all seasons, with significantly higher concentrations (WSRT, $p = 0.019$, $n = 22$) during the OND rains compared to the MAM rains. Dissolved CH_4 was consistently highest at the most upstream site across all seasons (Fig. 5b), decreasing rapidly downstream, with seasonal ranges of 4–3765 $\mu\text{mol L}^{-1}$, 5–4502 $\mu\text{mol L}^{-1}$ and 2–6729 $\mu\text{mol L}^{-1}$ recorded during the dry season, OND and MAM rain seasons, respectively.

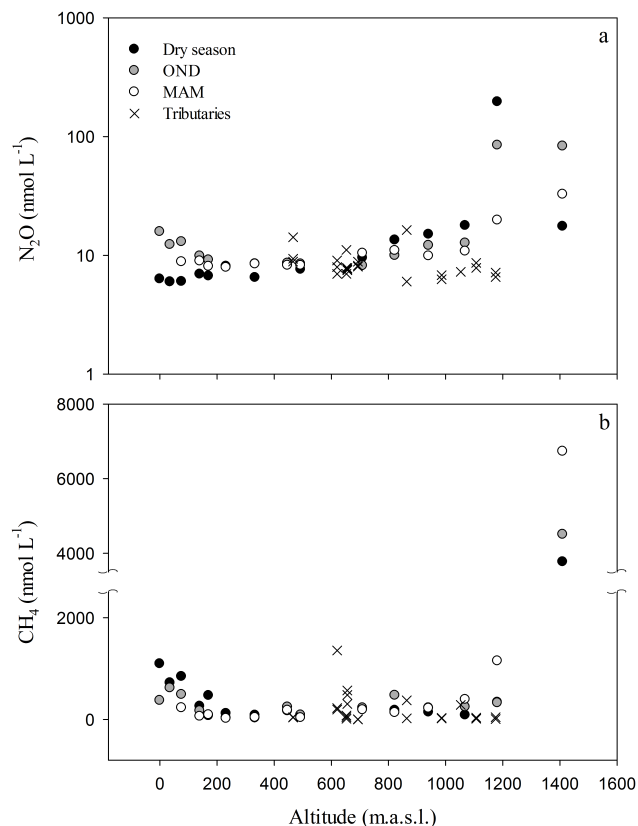


Fig. 5. Altitudinal gradient during dry season (August–September 2011), short rain season (October–December, OND, November 2011) and long rain season (March–May, MAM, April 2012) and tributaries (x, all seasons) of in-stream (a) dissolved N_2O (nmol L^{-1}), and (b) CH_4 (nmol L^{-1}).

$\delta^{15}\text{N}_{\text{PN}}$ displayed marked differences between the dry and rain seasons, with elevated $\delta^{15}\text{N}_{\text{PN}}$ signatures at most sites during the dry season (Fig. 6). $\delta^{15}\text{N}_{\text{PN}}$ signatures during the dry season (range: +3.1 to +31.5 ‰; mean: $+16.5 \pm 8.2$ ‰) were significantly elevated compared to both OND (range: -1.1 to +13.6 ‰; mean: $+7.3 \pm 2.6$ ‰; PTT, $p < 0.001$, $n = 19$) and MAM (range: 0.0 to +19.8 ‰; mean: $+7.6 \pm 5.9$ ‰; PTT, $p = 0.002$, $n = 19$) signatures. $\delta^{18}\text{O}_{\text{H}_2\text{O}}$ signatures during the MAM rains (range: -8.1 ‰ to -1.1 ‰; mean: -4.9 ± 2.1 ‰) were significantly lower compared to both the dry season (range: -5.3 ‰ to 0.6 ‰; mean: -2.4 ± 1.9 ‰) (PTT, $p < 0.001$, $n = 15$) and the OND rains (range: -5.5 ‰ to -1.1 ‰; mean: -2.8 ± 1.3 ‰) (PTT, $p = 0.001$, $n = 17$). Over a one-year sampling period at S20, a positive correlation was observed between $\delta^{18}\text{O}_{\text{H}_2\text{O}}$ and $\delta^{15}\text{N}_{\text{PN}}$ signatures (Pearson correlation, correlation coefficient = 0.436, $p = 0.0258$, $n = 26$) (Fig. 7).

Riverine POC:PN ratios varied between 5.3 and 21.2 (mean: 10.0 ± 3.6), 7.3 and 20.2 (10.4 ± 2.6), and 7.6 and 18.4 (11.9 ± 2.5) during the dry season, OND and MAM rains respectively. Riverine POC:PN ratios were signifi-

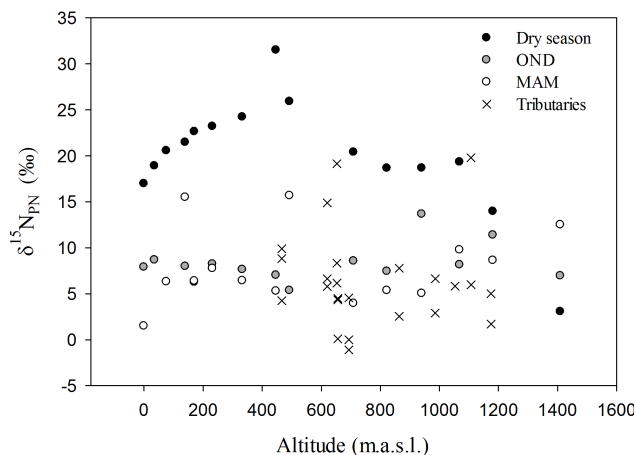


Fig. 6. Altitudinal gradient during dry season (August–September 2011), short rain season (October–December, OND, November 2011) and long rain season (March–May, MAM, April 2012) and all tributaries (x, all seasons) of in-stream $\delta^{15}\text{N}_{\text{PN}}$.

cantly higher during the MAM rains than both the dry season (PTT, $p = 0.01$, $n = 19$) and the OND rains (PTT, $p = 0.003$, $n = 23$). The POC:PN ratio generally increased downstream during the dry season and OND rains, with greater altitudinal variability displayed in the MAM rains, while tributaries usually displayed higher values than main channel sites of similar altitude.

Considerable variation was observed in pelagic PP and community R rates between the dry season and the two rain seasons, particularly in the lower reaches of the main channel (Fig. 8). However, 13 of 25 OND and 10 of 23 MAM PP measurements were below detection limits, recording < 1 ‰ change between initial and final $\delta^{13}\text{C}_{\text{POC}}$. Dry season R rates were significantly higher than during OND rains (PTT, $p = 0.001$, $n = 20$) and MAM rains (PTT, $p = 0.014$, $n = 18$).

4 Discussion

The disposal of untreated wastewater from the city of Nairobi has a profound impact on the A-G-S River network, leading to low O_2 levels, high NH_4^+ and high CH_4 at S1 in the Athi River. The highest CH_4 saturation level (336 440 ‰, April 2012 at S1) is well above published values in the main stream of other African rivers, such as 9600 ‰ in the Comoé River (Koné et al., 2010), 10 600 ‰ in the Bia River (Koné et al., 2010), 15 700 ‰ in the Tanoé River (Koné et al., 2010), and 8900 ‰ in the Oubangui River (Bouillon et al., 2012), and also relatively unpolluted temperate rivers such as the Ohio (10 000 ‰; Beaulieu et al., 2012). Yet, these CH_4 saturation values remain below those reported in the Amazon floodplains (up to 500 000 ‰; Richey et al., 1988; Bartlett et al., 1990). The high CH_4 saturation levels downstream of Nairobi are a signature of organic waste pollutants

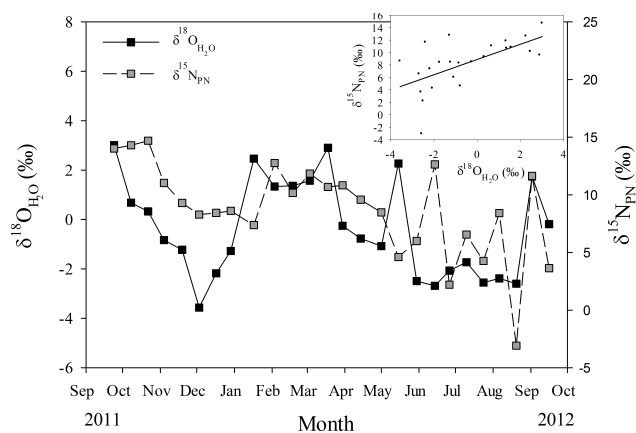


Fig. 7. A strong correlation was observed ($p = 0.0258$, $n = 26$) between $\delta^{18}\text{O}_{\text{H}_2\text{O}}$ and $\delta^{15}\text{N}_{\text{PN}}$ at S20 over a 12-month sampling period, with more elevated $\delta^{15}\text{N}_{\text{PN}}$ exported under drier conditions. (Inset) Linear regression of $\delta^{18}\text{O}_{\text{H}_2\text{O}}$ and $\delta^{15}\text{N}_{\text{PN}}$ with a one-month forward shift of $\delta^{18}\text{O}_{\text{H}_2\text{O}}$ ($y = 8.8888 + 1.2241x$; $r^2 = 0.3878$). The relationship weakens without the forward shift of $\delta^{18}\text{O}_{\text{H}_2\text{O}}$ ($y = -2.2256 + 0.2098x$; $r^2 = 0.1905$).

from sewage, as also observed in the vicinity of Abidjan with more modest CH_4 saturation levels of 20 000 % (Koné et al., 2010) and in the Adyar River, which is strongly polluted by the city of Chennai, with a massive CH_4 saturation level of 19 300 000 % (Rajkumar et al., 2008).

Water residence time exerts a major control on the quantity of N removed by streams and rivers, whereby a longer water residence time can increase physical (e.g. deposition) and biological nutrient cycling (e.g. nitrification, denitrification and primary production) (McGuire and McDonnell, 2007). This is evident in our data by the seasonal differences in longitudinal DIN profiles (Fig. 4a and b) of the A-G-S River network. During all seasons, urban wastewater discharge (as well as industrial point sources and agricultural runoff) in headwater tributaries have supplied the Athi River (site S1) with substantial quantities of DIN. During the peak of the hydrograph DIN is largely flushed (principally as NO_3^-) to the outlet, whereas during the trough of the hydrograph there should be decreased dilution of raw sewage inputs, which likely explains the higher N concentrations observed. The longer water residence time during the dry season would provide the basis for substantial removal of DIN above 450 m a.s.l. Though the lack of discharge data inhibits flux calculations, this should logically result in significantly lower DIN export to the ocean during the dry season.

Total alkalinity can increase in response to elevated ammonification rates (Abril and Frankignoulle, 2001) and intense NO_3^- removal by denitrification (Thomas et al., 2009), and through the intense assimilation of DIN by primary producers (Brewer and Goldman, 1976). Alternatively, TA decreases due to intense NH_4^+ removal by nitrification

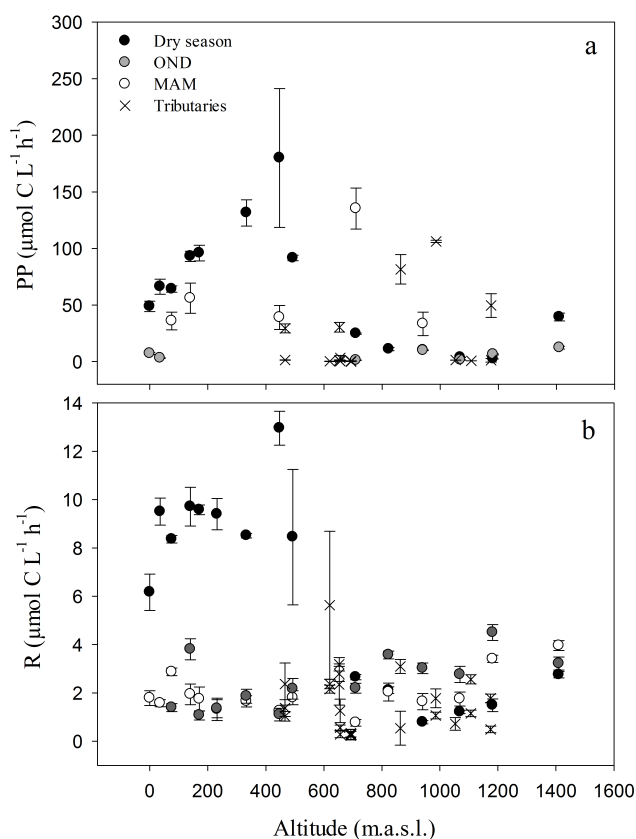


Fig. 8. Altitudinal gradient during dry season (August–September 2011), short rain season (October–December, OND, November 2011) and long rain season (March–May, MAM, April 2012) and tributaries (x, all seasons) of surface water (a) pelagic primary production (including error bars), and (b) community respiration rates (including error bars).

(Frankignoulle et al., 1996). The observed increase of TA between S1 and S2 ($2.16 \text{ mmol kg}^{-1}$ to $2.76 \text{ mmol kg}^{-1}$ respectively) during the dry season appears contrary to DIN observations of intense nitrification over this reach, where loss of NH_4^+ ($1012 \mu\text{mol L}^{-1}$) is closely mirrored by production of the NO_3^- ($856 \mu\text{mol L}^{-1}$), which should lead to a decrease in TA. The low POC : PN value of 5.3 at S1 is indicative of the upstream raw sewage inputs, while the loss of bulk POC before S2 (from 17.3 mg C L^{-1} to 3.9 mg C L^{-1}) suggests rapid mineralization of this material and production of NH_4^+ through ammonification. Production of 1 mmol of NH_4^+ by ammonification produces 1 mmol of TA (Abril and Frankignoulle, 2001), and, accordingly, the potential ammonification of the PN transformed between S1 and S2 (2.5 mg N L^{-1}) would increase TA by $0.18 \text{ mmol kg}^{-1}$, accounting for only 30 % of the observed increase. Meanwhile, pelagic PP decreases rapidly from $472 \mu\text{mol C L}^{-1} \text{ d}^{-1}$ at S1 to $29 \mu\text{mol C L}^{-1} \text{ d}^{-1}$ at S2, so we may assume it contributes insignificantly to the increase of TA by S2. However, water hyacinth (*Eichhornia crassipes*) was observed to completely

cover the dry season water surface over hundreds of metres between S1 and S2, and should be expected to significantly remove DIN and consequently increase TA, whereas these macrophytes were absent during the rain seasons when TA was observed to decrease over the corresponding reach. Notably, the rapid accumulation of N_2O (from 260 % saturation at S1 to 2855 % saturation at S2) suggests intense bacterial denitrification of available NO_3^- must be, in combination with ammonification and removal by macrophytes, the controlling factor increasing TA.

In addition to the NH_4^+ produced by the ammonification of PN between S1 and S2 during the dry season (potentially $179 \mu\text{mol } NH_4^+ \cdot N \text{ L}^{-1}$), a further $1012 \mu\text{mol L}^{-1}$ of the initial (entering at S1) NH_4^+ pool is transformed or lost from the system along this reach. To estimate NH_4^+ transformation and loss we employed a simple formula:

$$NH_4^+ \text{ loss} = (\Delta NH_4^+ + A_{NH_4^+}) / \left(\frac{D/V}{t} \right), \quad (3)$$

where ΔNH_4^+ is downstream change in NH_4^+ concentration ($\mu\text{mol L}^{-1}$), $A_{NH_4^+}$ equals the NH_4^+ produced by ammonification (assuming all PN is transformed to NH_4^+), D the distance (m) between the sites, V the average water velocity (dry season = 0.45 m s^{-1} , OND rains = 0.82 m s^{-1} , MAM rains = 1.16 m s^{-1} ; calculated from available discharge data between 1980 and 2008), and t a time factor to convert to a daily loss rate. Between S1 and S2 we estimate a NH_4^+ loss of $1248 \mu\text{mol N L}^{-1} \text{ d}^{-1}$. Based on in situ pelagic PP measurements at S1 and S2, and employing the Redfield C:N ratio, an estimated $4\text{--}71 \mu\text{mol N L}^{-1} \text{ d}^{-1}$ is removed by pelagic primary producers along the reach. If we assume NH_4^+ is solely utilised by primary producers over NO_3^- , pelagic PP accounts for only 0.3–5.7 % of the estimated NH_4^+ loss. The balance of NH_4^+ or NO_3^- uptake by primary producers is complex and often dependant on species composition and environmental conditions (Dortch, 1990), and even marginal NO_3^- uptake by pelagic PP will only decrease the percentage of NH_4^+ loss explained by this process. The strong enrichment of $\delta^{15}N_{PN}$, as discussed later, also points towards intense nitrification as the main factor controlling NH_4^+ removal. We hypothesise that NH_4^+ entering the study area at S1 (including NH_4^+ produced by ammonification between S1 and S2) is largely nitrified prior to S2, while unquantified (though considerable) NO_3^- removal by denitrification elevates N_2O saturation levels and, in conjunction with DIN removal by pelagic PP and floating macrophytes, increases TA. It is worth noting that the dense coverage of the water surface by macrophytes (predominantly *Eichhornia crassipes*) during the dry season (see supplementary material, Fig. S1) may inhibit the outgassing of N_2O to the atmosphere, thereby sustaining elevated N_2O saturation levels relative to periods of their absence, i.e. under conditions of higher discharge during the rain seasons.

Mean NO_3^- concentration observed in the A-G-S River over the three campaigns ($172.3 \pm 198.2 \mu\text{mol L}^{-1}$) is considerably higher relative to other African river catchments (Fig. 9; data not included in figure: Isinuka Springs, South Africa: $8.1 \mu\text{mol L}^{-1}$, Faniran et al., 2001; Berg River, South Africa: $1.1\text{--}13.4 \mu\text{mol L}^{-1}$, de Villiers, 2007; Comoé River, Ivory Coast, mean: $11.3 \pm 4.4 \mu\text{mol L}^{-1}$, Bia River, Ivory Coast, mean: $11.2 \pm 4.1 \mu\text{mol L}^{-1}$, Tanoé River, Ivory Coast, mean: $13.9 \pm 5.4 \mu\text{mol L}^{-1}$, Koné et al., 2009; Densu River, Ghana, mean: $33.4 \pm 0.2 \mu\text{mol L}^{-1}$, Fianko et al., 2010; Upper Ewaso Ng'iro River Basin, Kenya: $0.5\text{--}27.4 \mu\text{mol L}^{-1}$, Mutisya and Tole, 2010). The substantial NO_3^- loss observed between S2 and S13 during the dry season may be explained by pelagic PP assimilation of NO_3^- and/or removal by denitrifying bacteria. Assuming pelagic PP occurs only during daylight hours (12 h) and throughout the entire dry season water column (mean depth < 0.5 m), a basic comparison between daily in situ primary production rates and total NO_3^- loss can assist in identifying the more dominant process. A simple formula was employed for calculating daily NO_3^- loss ($\mu\text{mol } NO_3^- \text{ L}^{-1} \text{ d}^{-1}$) between consecutive sites:

$$NO_3^- \text{ Loss} = \Delta NO_3^- / \left(\frac{D/V}{t} \right), \quad (4)$$

where ΔNO_3^- is the concentration difference ($\mu\text{mol L}^{-1}$) between the upstream and downstream sites, D the distance (m) between the sites, V average water velocity (0.45 m s^{-1} ; calculated from available discharge data for 1980–2008 (late dry season months = August, September, October; $n = 85$) from gauging stations between S1 and S13), and t a time factor for converting to daily uptake rates. Again employing the Redfield C:N to convert PP carbon uptake to PP nitrogen uptake, it is clear that pelagic primary production cannot account for the considerable NO_3^- loss in these upper reaches (Table 1), although it becomes increasingly explanative downstream of S6. We have assumed here that pelagic PP is solely assimilating NO_3^- , opposite to nitrification loss calculations above, as any NH_4^+ assimilation will only decrease our estimate for removal of NO_3^- by primary producers. No *E. crassipes* blooms were observed over these reaches, and hence we assume the removal by in-stream macrophytes is minimal. Therefore, we hypothesise that the majority of NO_3^- formed from nitrification between S1 and S2 is removed over the following 240 km, initially by intense denitrification between S2 and S6, followed by considerable pelagic PP assimilation between S6 and S13.

N_2O is formed as a product of nitrification, the yield of N_2O production being a function of O_2 content (Goreau et al., 1980). Under strictly anoxic conditions, N_2O is removed through the denitrification pathway, but, in the presence of O_2 , denitrification leads to the accumulation of N_2O . While removal of N_2O through the denitrification pathway is a common feature in anoxic layers of lakes (Mengis et al., 1997),

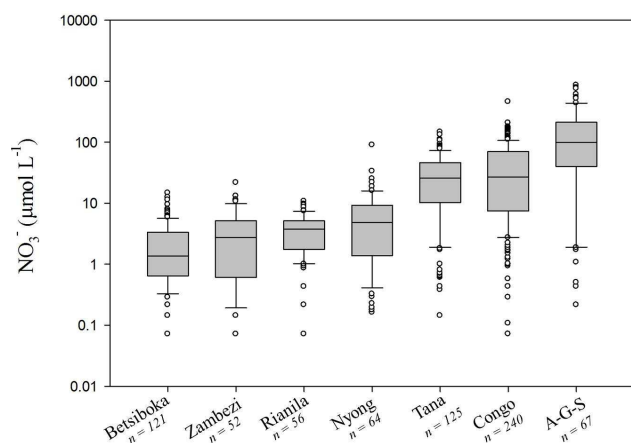


Fig. 9. Box plot of NO_3^- range for seven African river catchments. From left to right: Betsiboka catchment, Madagascar (own unpublished data); Zambezi catchment (own unpublished data); Rianila catchment, Madagascar (own unpublished data); Nyong catchment, Cameroon (Viers et al., 2000); Tana catchment, Kenya (Bouillon et al., 2009, and own unpublished data); Congo catchment (ORE-HYBAM and own unpublished data); and the Athi–Galana–Sabaki catchment, Kenya (data presented here). Further data sets included in text.

it has been less documented in rivers, where denitrification is assumed to be the principal source of N_2O (Beaulieu et al., 2011). For instance, Amazon floodplains were found to be sinks of atmospheric N_2O (Richey et al., 1988). In the highly polluted Adyar River, N_2O is also removed below atmospheric equilibrium by denitrification on some occasions (Rajkumar et al., 2008). Overall, the N_2O content in rivers is positively related to DIN (Zhang et al., 2010; Barnes and Upstill-Goddard, 2011; Baulch et al., 2011). The high N_2O content in the DIN-enriched Athi is consistent with these patterns. The only other published N_2O data set in African rivers also agrees with these patterns, as N_2O levels are close to atmospheric equilibrium in the Oubangui River (Bouillon et al., 2012) and characterized by low DIN values (mean NH_4^+ : $10.4 \pm 4.9 \mu\text{mol L}^{-1}$; mean NO_3^- : $4.2 \pm 4.4 \mu\text{mol L}^{-1}$; own unpublished data). It is not possible to discern the relative importance of N_2O production from nitrification and denitrification in the present data set, although we speculate that, in rivers strongly enriched in NH_4^+ due to lack of sewage treatment, nitrification may be a strong source of N_2O , unlike temperate rivers where DIN inputs are mainly due to NO_3^- leaching from cropland, and where denitrification is assumed to be the main source of N_2O (Beaulieu et al., 2011).

Particulate N in the Athi River at S1 has a $\delta^{15}\text{N}_{\text{PN}}$ value of $+3.1 \text{‰}$. The ammonification of the PN to NH_4^+ between S1 and S3, with a bias towards the lighter ^{14}N isotope being incorporated into the product, leads to the observed enrichment of the residual PN pool at S3 ($+19.3 \text{‰}$). Although we did not measure $\delta^{15}\text{N}$ of either the NH_4^+ or NO_3^- pool, we may expect the process of volatilization to lead to enrich-

Table 1. Inter-site comparison of average NO_3^- loss and pelagic primary production (PP)-assimilated N in order to delineate the primary control of NO_3^- loss for sites S2 to S13 during the dry season. The calculation of average NO_3^- loss is outlined in the discussion section. The range for PP-assimilated N is calculated using the upstream and downstream pelagic PP observations and converted from C uptake to N uptake using the Redfield C : N ratio. It must be stressed that these are basic calculations with a number of assumptions (see text).

Site	NO_3^- loss ($\mu\text{mol N L}^{-1} \text{d}^{-1}$)	PP-assimilated N ($\mu\text{mol N L}^{-1} \text{d}^{-1}$)	%N loss by PP
S2–S3	90	4–7	5–7
S3–S4	32	7–18	21–57
S4–S5	127	18–20	14–16
S5–S6	65	20–45	31–69
S6–S11	159	45–166	28–104
S11–S13	193	166–326	86–169

ment of the residual NH_4^+ pool, where, for example, Sebilo et al. (2006) measured a mean $\delta^{15}\text{N-NH}_4^+$ value of $9.5 \pm 1.7 \text{‰}$ in raw and treated wastewater of the Seine River, attributed to the volatilization of ^{15}N -depleted NH_4^+ . Isotope fractionation factors for nitrification, -20‰ in the Seine River for example (Sebilo et al., 2006), suggest the $\delta^{15}\text{N-NH}_4^+$ pool will become increasingly enriched in ^{15}N through the conversion of NH_4^+ to NO_3^- . As such, following ammonification of PN, volatilization, and nitrification of NH_4^+ , we can expect the residual DIN pools to be heavily enriched in ^{15}N , and, although we have no direct measurements, Kreitler (1979) suggest the conversion of animal waste (with a $\delta^{15}\text{N}$ value of about $+5 \text{‰}$) to NO_3^- results in $\delta^{15}\text{N}$ values generally between $+10 \text{‰}$ and $+20 \text{‰}$.

We observed minimal change in $\delta^{15}\text{N}_{\text{PN}}$ values between S3 and S6, which may be explained by the lack of assimilation of DIN by phytoplankton in the water column, evidenced by the low primary production rates outlined above. Additionally, the intense denitrification between S3 and S6 may not result in further significant alteration to riverine $\delta^{15}\text{N}$ values of NO_3^- , as previous studies indicate that minimal fractionation (-1.5‰ to -3.6‰) occurs during benthic denitrification as the water–sediment interface diffusion of NO_3^- is the rate-limiting step, which in itself causes little fractionation (Sebilo et al., 2003; Lehmann et al., 2004).

The enrichment of $\delta^{15}\text{N}_{\text{PN}}$ between S6 and S13 during the dry season may be attributed to the pelagic assimilation of the residual ^{15}N -enriched DIN by primary producers, as shown by Cole et al. (2004), who found a strong correlation between the relative contribution of wastewater to stream flow and ^{15}N values of aquatic primary producers. The higher %POC and low POC : PN observed over these sites are consistent with the presence of high phytoplankton biomass and, although logistical constraints did not allow

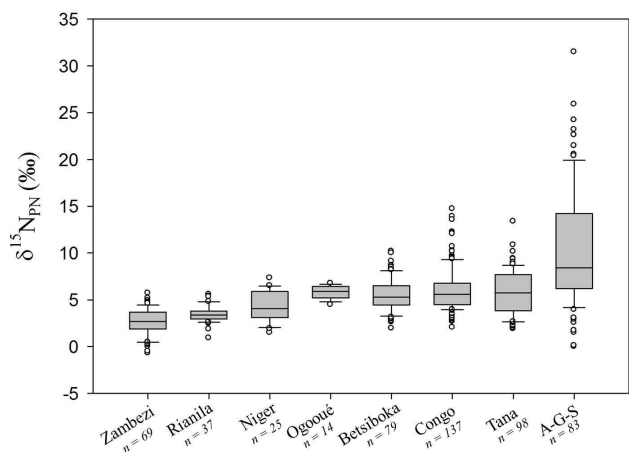


Fig. 10. Box plot of the range of $\delta^{15}\text{N}_{\text{PN}}$ data for seven African river catchments. From left to right: Zambezi catchment, Zambia and Mozambique (Zurbrügg et al., 2013, and own unpublished data); Rianila catchment, Madagascar (own unpublished data); Niger catchment, Niger (own unpublished data); Ogooué Catchment, Gabon (own unpublished data); Betsiboka catchment, Madagascar (own unpublished data); Congo catchment, Central African Republic and Democratic Republic of the Congo (own unpublished data); Tana catchment, Kenya (Bouillon et al., 2009, and own unpublished data); and the Athi–Galana–Sabaki catchment, Kenya (data presented here).

for Chl *a* measurement, the water along these reaches was stained a characteristic green hue (see supplementary material, Fig. S2). These findings are consistent with di Persia and Neiff (1986), who suggest that highest phytoplankton biomass density in tropical rivers occurs during the dry season, when water residence time is greatest and turbidity is minimal, with similar patterns also observed in tropical rivers of the Ivory Coast (Lévêque, 1995; Koné et al., 2009), Asia (Dudgeon, 1995) and Australia (Townsend et al., 2011). By S13 a combination of intense denitrification (between S3 and S6) and high pelagic primary production (between S6 and S13) lowers NO_3^- concentration to a level equivalent with other African river catchments (see Fig. 9), whilst the latter process simultaneously leads to elevated $\delta^{15}\text{N}_{\text{PN}}$ values not previously recorded in African river catchments (Fig. 10).

Between S13 and S20 pelagic primary production rates gradually decline with a concomitant decrease in %POC and $\delta^{15}\text{N}_{\text{PN}}$, and increasing POC : PN. Following the confluence of the Tsavo with the Athi River upstream of S14, there are no further tributaries during the dry season contributing discharge to the drainage network, and therefore the above observations are not a consequence of gradual dilution by additional inputs, but rather in-stream transformation of C and N pools. We identify two broad sources of TSM in the A-G-S system: a terrestrially sourced TSM with characteristically low %POC and high POC : PN, and an autochthonous TSM source in the form of algal biomass, represented by high %POC and low POC : PN. Our most likely hypothesis

to explain the downstream trends in %POC, POC / PN, and $\delta^{15}\text{N}_{\text{PN}}$ signatures is the preferential loss of the more labile, ^{15}N -enriched algal biomass pool.

In order to test this hypothesis, we attempted to fit a two-source mixing model to field observations between S13 and S20, where a pure autochthonous source was defined by %POC of 40, POC : PN represented by the Redfield ratio, and a $\delta^{15}\text{N}_{\text{PN}}$ of +32 ‰, a value marginally elevated relative to the highest field observations (+31.5 ‰ at S13). Under dry season conditions, we would expect minimal contribution of soil erosion to the terrestrial source, whereas much of the dry season OC may be sourced from upstream organically enriched wastewater discharge. The best fit to the data was found by employing a terrestrial POC : PN of 18, i.e. considerably lower than reported terrestrial C : N ratios (e.g. mean = 36; Elser et al., 2000) but in line with expected degradation within the aquatic system, and a terrestrial $\delta^{15}\text{N}_{\text{PN}}$ of +5 ‰. Assuming an initial proportion of autochthonous:terrestrial sourced TSM of 85 : 15, and simulating the effect of gradual decomposition of the labile (autochthonous) component while the (less labile) terrestrial component remained intact and in transit, the mixing model output provided a good relationship with observed POC : PN and $\delta^{15}\text{N}_{\text{PN}}$ (Fig. 11a). Likewise, a suitable match is established between field observations and mixing model output for %POC and $\delta^{15}\text{N}_{\text{PN}}$ (Fig. 11b) when employing the above constraints and a terrestrial %POC end member of 8. Although the terrestrial %POC end member is relatively high, it provides the best fit with field observations in this situation and can be partially justified by the high organic loading in the headwaters.

We speculate that the preferential decomposition of more labile autochthonous organic matter, relative to more recalcitrant terrestrial materials, is largely driving the %POC lower and POC : PN ratio higher along this lower reach, which in turn leads to depletion of ^{15}N within the PN pool. Bouillon et al. (2009) and Tamooh et al. (2012) reported similar rapid loss of phytoplankton biomass in the bordering Tana River catchment, as did Zurbrügg et al. (2013) in the Kafue River, Zambia, albeit downstream of reservoirs in both these studies. As the quantity of (^{15}N -enriched) phytoplankton biomass decreases in the A-G-S, the PN gradually becomes more depleted in ^{15}N , though still discharging to the Indian Ocean a $\delta^{15}\text{N}$ signature (+17.0 ‰) evidently imprinted by upstream wastewater inputs.

As outlined earlier, the A-G-S catchment has undergone considerable land use change in the past century, largely as a result of increased population pressure and associated resource demands placed on the region. Ba / Ca ratios in Malindi reef corals, collected from the coastal surroundings of the A-G-S catchment, have been employed to reconstruct a 300 yr timeline of increasing sediment flux to the ocean (Fleitmann et al., 2007), linked to exacerbated soil erosion associated with intensified land use, cultivation of steep slopes, deforestation for wood fuel production, urban sprawl and expanding rural (predominantly unsealed) road networks

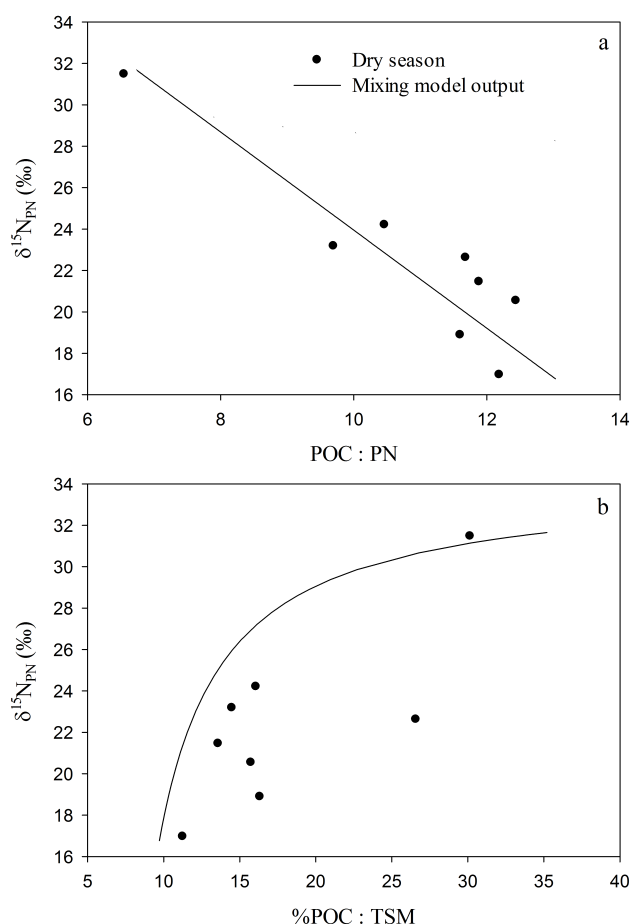


Fig. 11. Field measurements between S13 and S20 and mixing model output (solid line) for (a) POC : PN and $\delta^{15}\text{N}_{\text{PN}}$, showing the preferential metabolism of phytoplankton biomass and associated depletion of the $\delta^{15}\text{N}_{\text{PN}}$ pool downstream of the observed phytoplankton blooms. The non-linear relationship between (b) %POC and $\delta^{15}\text{N}_{\text{PN}}$ supports the suggestion of rapid removal of the labile phytoplankton biomass downstream of S13.

throughout the catchment. Ohowa (1996), similar to our results, observed peaks in NO_3^- concentration at the A-G-S outlet during the MAM and OND rains, though their peak NO_3^- measurement ($1.4 \mu\text{mol L}^{-1}$; 1991 OND rains) was more than two magnitudes lower than our peak observation ($530.7 \mu\text{mol L}^{-1}$; 2011 OND rains) two decades later. The reason for discrepancy between results is ambiguous. Assuming no measurement error on the part of Ohowa (1996), we may interpret the difference as a very rapid increase of NO_3^- export from the A-G-S catchment over the last 20 yr. The insufficient development of sewage and sanitation services to match the burgeoning Nairobi population, having more than doubled over the two decades between work of Ohowa (1996) and the present study, is a likely contributor to the substantial increase observed in NO_3^- export.

The Global News2 model (Mayorga et al., 2010) predicts TSM and PN loads of approximately 38.76 Tg yr^{-1} and $16.44 \text{ Gg N yr}^{-1}$ for the A-G-S outlet respectively, equating to 0.04 %PN. This is considerably less than the average value of 0.31 %PN calculated for our measurements over a one-year sampling period ($n = 28$). Mayorga et al. (2010) first estimate TSM load and then use empirical relationships observed between TSM and %PN to estimate the PN load. Local conditions of N loading in the A-G-S system, as outlined above, are not considered in the Global News2 estimates, which may explain the discrepancy between the model output and our field-derived observations. Hence, caution should prevail when employing these broad-scale modelling relationships to heavily disturbed systems such as the A-G-S catchment.

Bi-weekly data gathered at the most downstream station (S20) show large annual $\delta^{15}\text{N}_{\text{PN}}$ fluctuation, which we suggest is related to a seasonally variable river water source, namely, variable contributions from precipitation and groundwater. As corresponding discharge measurements were unavailable, we used $\delta^{18}\text{O}$ values of river water ($\delta^{18}\text{O}_{\text{H}_2\text{O}}$), a seasonally variable mix of precipitation and groundwater, as a proxy for river discharge. Around Nairobi (Station # 6374101, $\sim 1700 \text{ m a.s.l.}$; IAEA, 2001), mean dry season (June–September) $\delta^{18}\text{O}$ values of precipitation ($-2.1 \pm 0.9 \text{ ‰}$) are considerably elevated compared to precipitation during the MAM ($-5.1 \pm 1.4 \text{ ‰}$) and OND ($-5.1 \pm 1.2 \text{ ‰}$) wet seasons. $\delta^{18}\text{O}$ of precipitation is affected by the altitude of rainout also, with Clark and Fritz (1997) reporting a global range of -0.15 ‰ to -0.5 ‰ per 100 m increase in elevation. Using a mid-value of their range (-0.3 ‰ per 100 m increase in elevation), $\delta^{18}\text{O}$ of precipitation in the lower catchment (e.g. 200 m a.s.l.) may increase toward $\sim +2 \text{ ‰}$ during the dry months and $\sim -1 \text{ ‰}$ over the wet seasons. During the dry season, baseflow is predominantly composed of groundwater recharge, which is, relative to precipitation, isotopically enriched in ^{18}O due to evaporative processes following rainout. During rain seasons the groundwater $\delta^{18}\text{O}$ signature becomes diluted by the lower $\delta^{18}\text{O}$ of catchment precipitation (Mook and De Vries, 2000), consequently depleting river water in ^{18}O in comparison to drier months.

Following from these observations, we can use riverine $\delta^{18}\text{O}_{\text{H}_2\text{O}}$ data as a reasonable proxy of river discharge, where higher $\delta^{18}\text{O}$ indicates drier climatic conditions and decreasing $\delta^{18}\text{O}$ is representative of increasing contribution of precipitation to discharge. Comparing riverine $\delta^{18}\text{O}_{\text{H}_2\text{O}}$ with $\delta^{15}\text{N}_{\text{PN}}$ values at the outlet of the A-G-S River over the course of a year, we find the two isotope signatures largely increase and decrease in unison (Fig. 7). A more acceptable linear fit was found by shifting the $\delta^{18}\text{O}_{\text{H}_2\text{O}}$ observations forward one month relative to $\delta^{15}\text{N}_{\text{PN}}$ observations, which may be a temporal delay associated with N cycle processes as a result of the changing hydrograph (e.g. time required for sufficient assimilation of ^{15}N -enriched PN to be observed within

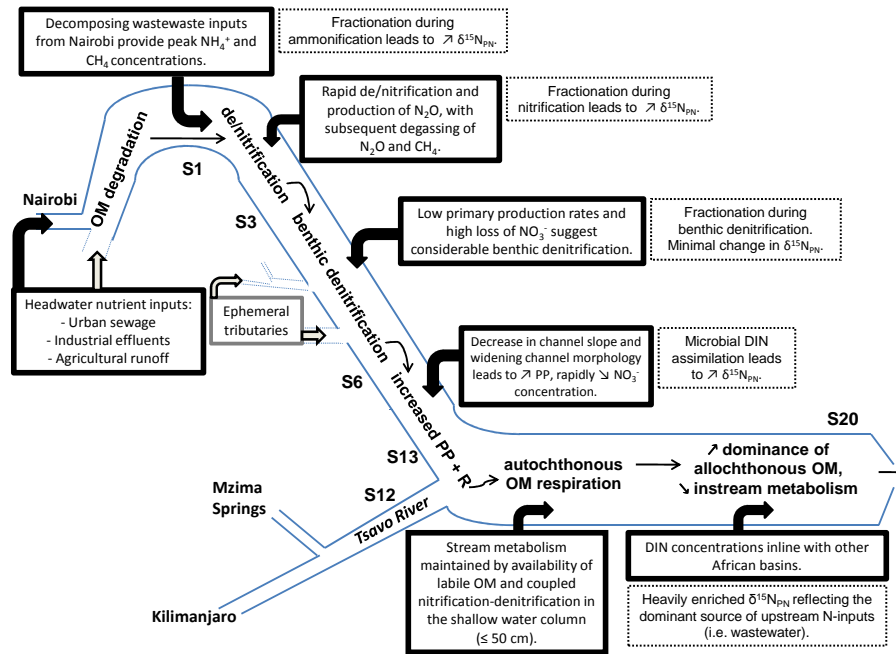


Fig. 12. Conceptual scheme of dry season N cycling in the A-G-S River catchment, Kenya. (Upper left) Surface runoff and direct input of organic wastes in the upper catchment provide large quantities of DIN at S1, much of which has been transformed and removed from the aquatic system below S13. Dominant processes and river characteristics along each reach (bold boxes with arrow) are outlined, as well as downstream evolution of the $\delta^{15}\text{N}_{\text{PN}}$ signature (dashed boxes).

the PN pool). From this we can see that the export of PN enriched in ^{15}N during the dry season compared to export of relatively ^{15}N -depleted PN during rain seasons clearly highlights the annual variability of N cycling in the A-G-S system and its link with water residence time.

Our $\delta^{15}\text{N}_{\text{PN}}$ data highlight the impact of human-induced disturbance on the N cycle within the A-G-S catchment. Accordingly, potential exists for employing the $\delta^{15}\text{N}$ values of sediments, bivalves and corals from within the catchment and marine environment surrounding the river mouth as proxies for the historical evolution of N sources to the A-G-S catchment. Elliot and Bush (2006) related an increase in $\delta^{15}\text{N}_{\text{org}}$ values from +2‰ to +7‰ in a freshwater wetland sediment core spanning 350 yr to changes in land use from forested conditions to increasing nutrient inputs from human wastes. According to Marion et al. (2005), the coring of coral heads and extraction of $\delta^{15}\text{N}$ values could provide timelines extending from centuries to millennia. Others have found that the $\delta^{15}\text{N}$ values in the growth tips of Gorgonians (coral fans) closely reflect the food (N) source of the organism (Risk et al., 2009), with many species forming annual growth rings (Grigg, 1974) which can remain chemically stable for a period of time following death (Goldberg and Hamilton, 1974; Goldberg, 1976; Sherwood et al., 2005). Similarly, the growth pattern of bivalves provides a timeline of the evolution of the organisms' external environment, with potential preservation of the organic matrix for

thousands of years (Weiner et al., 1979; Risk et al., 1997). With species-specific lifespans exceeding 50 yr, an organism may store proxies of pre-disturbance terrestrial conditions in currently disturbed environments. With the proximity of Malindi–Watamu reef to the A-G-S outlet, there should exist a plethora of submerged marine biological proxies which could assist in creating a $\delta^{15}\text{N}$ timeline of land use change within the A-G-S catchment. The sediment-laden nature of the A-G-S River and the associated infilling of the Sabaki estuary, first recognized by Oosterom (1988), may also store a comprehensive $\delta^{15}\text{N}$ timeline of N evolution in the catchment. The relatively low-cost nature of these techniques is an added benefit for their use in economically challenged, developing countries where little baseline data exist (Risk et al., 2009).

5 Conclusions

Nitrogen loading of the A-G-S headwaters surrounding Nairobi leads to large seasonal N-cycling dynamics within the catchment. High discharge during rain seasons results in the rapid flushing of large quantities of DIN from the headwaters to the outlet, whereas we speculate that increased water residence time during the dry season permits substantial transformation and removal of DIN in the upper to mid-catchment (Fig. 12). The decomposition of wastewater inputs during the dry season provides a large volume of DIN which

undergoes intense nitrification in the upper reaches, producing elevated NO_3^- concentrations, significant N_2O and elevated $\delta^{15}\text{N}_{\text{PN}}$, while concomitant denitrification leads to further N_2O outgassing to the atmosphere. Over the following 240 km, a combination of benthic denitrification and pelagic primary production efficiently lower NO_3^- levels to the range observed in most other African catchments, whilst associated fractionation further enriches $\delta^{15}\text{N}_{\text{PN}}$. Availability of labile OM and coupled nitrification–denitrification in the shallow water column maintains elevated in-stream metabolism in the lower reaches, with the river discharging significantly diminished DIN concentrations, relative to upstream inputs, during the dry season. The strong correlation found between seasonal $\delta^{15}\text{N}_{\text{PN}}$ and river discharge presents the possibility of employing mutually beneficial proxy indicators – such as a combination of $\delta^{15}\text{N}_{\text{PN}}$ of sediments, corals and bivalves – to build the foundation of how historical land use changes have influenced N cycling within the catchment.

Supplementary material related to this article is available online at <http://www.biogeosciences.net/11/443/2014/bg-11-443-2014-supplement.zip>.

Acknowledgements. Funding for this work was provided by the European Research Council (ERC-StG 240002, AFRIVAL, <http://ees.kuleuven.be/project/afriaval/>), and by the Research Foundation Flanders (FWO-Vlaanderen, project G.0651.09). We thank Z. Kelemen (KU Leuven), P. Salaets (KU Leuven), and M.-V. Commarieu (ULg) for technical and laboratory assistance, M. Kioko (Kenya Wildlife Service) for field assistance during the seasonal sampling campaigns, and J. Ngilu and W.R.M.A. (Water Resource Management Authority, Machakos, Kenya) for providing the discharge data for various A-G-S gauging stations. Data in the Ogooué (Gabon) were collected by J.-D. Mbega (Institut de Recherches Agronomiques et Forestières, Libreville, Gabon) and data in the Niger were collected by A. Bassirou (Univerté de Niamey, Niamey, Niger). A. V. Borges is a senior research associate at the FRS-FNRS (Belgium). We thank B. Mayer and an anonymous reviewer for their insightful and constructive comments on an earlier draft of this manuscript.

Edited by: N. Ohte

References

- Abril, G. and Frankignoulle, M.: Nitrogen–alkalinity interactions in the highly polluted Scheldt basin (Belgium), *Water Res.*, 35, 844–850, 2001.
- Aravena, R., Evans, M. L., and Cherry, J. A.: Stable isotopes of oxygen and nitrogen in source identification of nitrate from septic systems, *Ground Water*, 31, 180–186, 1993.
- Ayres, R. U., Schlesinger, W. H., and Socolow, R. H.: Human impacts on the nitrogen cycle, in: *Industrial Ecology and Global Change*, edited by: Socolow, R., Andrews, C., Berkhout, F., and Thomas, V., Cambridge University Press, Cambridge, United Kingdom, 121–155, 1994.
- Bartlett, K. B., Crill, P. M., Bonassi, J. A., Richey, J. E., and Harris, R. C.: Methane flux from the Amazon River floodplain: emissions during rising water, *J. Geophys. Res.*, 95, 16773–16778, doi:10.1029/JD095iD10p16773, 1990.
- Barnes, J. and Upstill-Goddard, R. C.: N_2O seasonal distributions and air-sea exchange in UK estuaries: implications for the tropospheric N_2O source from European coastal waters, *J. Geophys. Res.*, 116, G01006, doi:10.1029/2009JG001156, 2011.
- Baulch, H. M., Schiff, S. L., Maranger, R., and Dillon, P. J.: Nitrogen enrichment and the emission of nitrous oxide from streams, *Global Biogeochem. Cy.*, 25, GB4013, doi:10.1029/2011GB004047, 2011.
- Beaulieu, J. J., Tank, J. L., Hamilton, S. K., Wollheim, W. M., Hall Jr., R. O., Mulholland, P. J., Peterson, B. J., Ashkenas, L. R., Cooper, L. W., Dahm, C. N., Dodds, W. K., Grimm, N. B., Johnson, S. L., McDowell, W. H., Poole, G. C., Valett, H. M., Arango, C. P., Bernot, M. J., Burgin, A. J., Crenshaw, C. L., Helton, A. M., Johnson, L. T., O'Brien, J. M., Potter, J. D., Sheibley, R. W., Sobota, D. J., and Thomas, S. M.: Nitrous oxide emission from denitrification in stream and river networks, *P. Natl. Aca. Sci.*, 108, 214–219, 2011.
- Beaulieu, J. J., Shuster, W. D., and Rebolz, J. A.: Controls on gas transfer velocities in a large river, *J. Geophys. Res.*, 117, G02007, doi:10.1029/2011JG001794, 2012.
- Bouillon, S., Abril, G., Borges, A. V., Dehairs, F., Govers, G., Hughes, H. J., Merckx, R., Meysman, F. J. R., Nyunja, J., Osburn, C., and Middelburg, J. J.: Distribution, origin and cycling of carbon in the Tana River (Kenya): a dry season basin-scale survey from headwaters to the delta, *Biogeosciences*, 6, 2475–2493, doi:10.5194/bg-6-2475-2009, 2009.
- Bouillon, S., Yambélé, A., Spencer, R. G. M., Gillikin, D. P., Hernes, P. J., Six, J., Merckx, R., and Borges, A. V.: Organic matter sources, fluxes and greenhouse gas exchange in the Oubangui River (Congo River basin), *Biogeosciences*, 9, 2045–2062, doi:10.5194/bg-9-2045-2012, 2012.
- Bouwman, A. F., Van Drecht, G., Knoop, J. M., Beusen, A. H. W., and Meinardi, C. R.: Exploring changes in river nitrogen export to the world's oceans, *Global Biogeochem. Cy.*, 19, GB1002, doi:10.1029/2004GB002314, 2005.
- Brewer, P. G. and Goldman, J. C.: Alkalinity changes generated by phytoplankton growth, *Limnol. Oceanogr.*, 21, 108–117, 1976.
- Canfield, D. E., Glazer, A. N., and Falkowski, P. G.: The evolution and future of Earth's nitrogen cycle, *Science*, 330, 192–196, doi:10.1126/science.1186120, 2010.
- Cao, H., Auguet, J.-C., and Gu, J.-D.: Global ecological pattern of ammonia-oxidizing archaea, *PLoS ONE*, 8, e52853, doi:10.1371/journal.pone.0052853, 2013.
- Caraco, N. F. and Cole, J. J.: Human impact on nitrate export: an analysis using major world rivers, *Ambio*, 28, 167–170, 1999.
- Carpenter, S. R., Caraco, N. F., Correll, D. L., Howarth, R. W., Sharpley, A. N., and Smith, V. H.: Nonpoint pollution of surface waters with phosphorus and nitrogen, *Ecol. Appl.*, 8, 559–568, 1998.
- Clark, I. D. and Fritz, P.: *Environmental Isotopes in Hydrogeology*, Lewis Publishers, Boca Raton, FL., 1997.

- Cole, M. L., Valiela, I., Kroeger, K. D., Tomasky, G. L., Cebrian, J., Wigand, C., McKinney, R. A., Grady, S. P., and Carvalho da Silva, M. H.: Assessment of a $\delta^{15}\text{N}$ isotopic method to indicate anthropogenic eutrophication in aquatic ecosystems, *J. Environ. Qual.*, 33, 124–132, 2004.
- Costanzo, S. D., O'donohue, M. J., Dennison, W. C., Loneragan, N. R., and Thomas, M.: A new approach for detecting and mapping sewage impacts, *Mar. Pollut. Bull.*, 42, 149–156, 2001.
- Dafe, F.: No business like slum business? The political economy of the continued existence of slums: a case study of Nairobi, DES-TIN: Development Studies Institute, Working Paper Series, No. 09–98, 2009.
- De Brabandere, L., Dehairs, F., Van Damme, S., Brion, N., Meire, P., and Daro, N.: $\delta^{15}\text{N}$ and $\delta^{13}\text{C}$ dynamics of suspended organic matter in freshwater and brackish waters of the Scheldt estuary, *J. Sea Res.*, 48, 1–15, 2002.
- de Villiers, S.: The deteriorating nutrient status of the Berg River, South Africa, *Water SA*, 33, 659–664, 2007.
- di Persia, D. H. and Neiff, J. J.: The Uruguay river system, in: *The ecology of river systems*, edited by: Davies, B. R., Walker K. F., and Junk, W., Dordrecht, the Netherlands, 599–662, 1986.
- Dortch, Q.: The interaction between ammonium and nitrate uptake in phytoplankton, *Marine ecology progress series*, Oldendorf, 61, 183–201, 1990.
- Downing, J. A., McClain, M., Twilley, R., Melack, J. M., Elser, J., Rabalais, N. N., Lewis, Jr., W. M., Turner, R. E., Corredor, J., Soto, D., Yanez-Arancibia, A., Kopaska, J. A., and Howarth, R. W.: The impact of accelerating land-use change on the N-cycle of tropical aquatic ecosystems: current conditions and projected changes, *Biogeochemistry*, 46, 109–148, 1999.
- Dudgeon, D.: The ecology of rivers and streams in tropical Asia, in: *River and stream ecosystems*, edited by: Cushing, C. E., Cummins, K. W., and Minshall, G. W., Elsevier Science B. V., Amsterdam, 615–657, 1995.
- Elliot, E. M. and Brush, G. S.: Sedimented organic nitrogen isotopes in freshwater wetlands record long-term changes in watershed nitrogen source and land use, *Environ. Sci. Technol.*, 40, 2910–2916, 2006.
- Elser, J. J., Fagan, W. F., Denno, R. F., Dobberfuhr, D. R., Folarin, A., Huberty, A., Interlandi, S., Kilham, S. S., McCauley, E., Schulz, K. L., Siemann, E. H., and Sterner, R. W.: Nutritional constraints in terrestrial and freshwater food webs, *Nature*, 408, 578–580, 2000.
- Faniran, J. A., Ngceba, F. S., Bhat, R. B., and Oche, C. Y.: An assessment of the water quality of the Isinuka springs in the Transkei region of the Eastern Cape, Republic of South Africa, *Water SA*, 27, 241–250, 2001.
- Fianko, J. R., Lowor, S. T., Donkor, A., and Yeboah, P. O.: Nutrient chemistry of the Densu River in Ghana, *The Environmentalist*, 30, 145–152, 2010.
- Fleitmann, D., Dunbar, R. B., McCulloch, M., Mudelsee, M., Vuille, M., McClanahan, T. R., Cole, J. E., and Eggins, S.: East African soil erosion recorded in a 300 year old coral colony from Kenya, *Geophys. Res. Lett.*, 34, L04401, doi:10.1029/2006GL028525, 2007.
- Frankignoulle, M., Bourge, I., and Wollast, R.: Atmospheric CO_2 fluxes in a highly polluted estuary (The Scheldt), *Limnol. Oceanogr.*, 41, 365–369, 1996.
- French, E., Kozłowski, J. A., Mukherjee, M., Bullerjahn, G., and Bollmann, A.: Ecophysiological characterization of ammonia-oxidizing archaea and bacteria from freshwater, *Appl. Environ. Microb.*, 78, 5773–5780, 2012.
- Galloway, J. N. and Cowling, E. B.: Reactive nitrogen and the world: 200 years of change, *AMBIO*, 31, 64–71, 2002.
- Galloway, J. N., Schlesinger, W. H., Hiram Levy, I. I., Michaels, A., and Schnoor, J. L.: Nitrogen fixation: anthropogenic enhancement-environmental response, *Global Biogeochem. Cy.*, 9, 235–252, 1995.
- Galloway, J. N., Aber, J. D., Erisman, J. W., Seitzinger, S. P., Howarth, R. W., Cowling, E. B., and Cosby, B. J.: The nitrogen cascade, *BioScience*, 53, 341–356, 2003.
- Gillikin, D. P. and Bouillon, S.: Determination of $\delta^{18}\text{O}$ of water and $\delta^{13}\text{C}$ of dissolved inorganic carbon using a simple modification of an elemental analyser-isotope ratio mass spectrometer: an evaluation, *Rapid Commun. Mass Sp.*, 21, 1475–1478, 2007.
- Goldberg, W. M.: Comparative study of the chemistry and structure of gorgonian and antipatharian coral skeletons, *Mar. Biol.*, 35, 253–267, 1976.
- Goldberg, W. M. and Hamilton, R. D.: The sexual cycle in *Plexaura homomalla*, in: *Prostaglandins from Plexaura homomalla: ecology, utilization and conservation of a major medical marine resource*. A Symposium, edited by: Bayer, M. and Weinheimer, A. J., University of Miami Press, Miami, FL, 58–61, 1974.
- Goreau, T. J., Kaplan, W. A., Wofsy, S. C., McElroy, M. B., Valois, F. W., and Watson, S. W.: Production of NO_2^- and N_2O by nitrifying bacteria at reduced concentrations of oxygen, *Appl. Environ. Microbiol.*, 40, 526–532, 1980.
- Grigg, R. W.: Growth rings: annual periodicity in two gorgonian corals, *Ecology*, 55, 876–881, 1974.
- Hama, T., Miyazaki, T., Ogawa, Y., Iwakuma, T., Takahashi, M., Otsuki, A., and Ichimura, S.: Measurement of photosynthetic production of a marine phytoplankton population using a stable ^{13}C isotope, *Mar. Biol.*, 73, 31–36, 1983.
- Harrison, J. A., Maranger, R. J., Alexander, R. B., Giblin, A. E., Jacinthe, P. A., Mayorga, E., Seitzinger, S. P., Sobota, D. J., and Wollheim, W. M.: The regional and global significance of nitrogen removal in lakes and reservoirs, *Biogeochemistry*, 93, 143–157, 2009.
- Holland, E. A., Dentener, F. J., Braswell, B. H., and Sulzman, J. M.: Contemporary and pre-industrial global reactive nitrogen budgets, *Biogeochemistry*, 46, 7–43, 1999.
- Howarth, R. W.: Coastal nitrogen pollution: a review of sources and trends globally and regionally, *Harmful Algae*, 8, 14–20, 2008.
- Howarth, R. W., Billen, G., Swaney, D., Townsend, A., Jaworski, N., Lajtha, K., Downing, J. A., Elmgren, R., Caraco, N., Jordan, T., Berendse, F., Freney, J., Kudeyarov, V., Murdoch, P., and Zhao-Liang, Z.: Regional nitrogen budgets and riverine N and P fluxes for the drainages to the North Atlantic Ocean: natural and human influences, *Biogeochemistry*, 35, 75–139, 1996.
- Hugoni, M., Etien, S., Bourges, A., Lepère, C., Domaizon, I., Mallet, C., Bronner, G., Debroyas, D., and Mary, I.: Dynamics of ammonia oxidizing archaea and bacteria in contrasted freshwater ecosystems, *Res. Microbiol.*, 164, 360–370, doi:10.1016/j.resmic.2013.01.004, 2013.
- IAEA: GNIP Maps and Animations, International Atomic Energy Agency, Vienna, <http://isohis.iaea.org> (last accessed: 25 November 2013), 2001.

- K.N.B.S.: Kenya: 2009 population and housing census highlights, Kenyan National Bureau of Statistics, 2009.
- Kithiia, S. M.: Land use changes and their effects on sediment transport and soil erosion within the Athi drainage basin, Kenya, IAHS-AISH P., 245, 145–150, 1997.
- Kithiia, S. M.: Effects of Sediments Loads on Water Quality within the Nairobi River Basins, Kenya, International Journal of Environmental Protection, 2, 16–20, 2012.
- Kithiia, S. M. and Wambua, B. N.: Temporal changes of sediment dynamics within the Nairobi River sub-basins between 1998–2006 time scale, Kenya, Annals of Warsaw University of Life Sciences – SGGW, Land Reclamation, 42, 17–22, 2010.
- Koné, Y. J. M., Abril, G., Kouadio, K. N., Delille, B., and Borges, A. V.: Seasonal variability of carbon dioxide in the rivers and lagoons of Ivory Coast (West Africa), Estuaries and Coasts, 32, 246–260, 2009.
- Koné Y. J. M., Abril, G., Delille, B., and Borges, A. V.: Seasonal variability of methane in the rivers and lagoons of Ivory Coast (West Africa), Biogeochemistry, 100, 21–37, 2010.
- Kreitler, C. W.: Nitrogen-isotope ratio studies of soils and groundwater nitrate from alluvial fan aquifers in Texas, J. Hydrol., 42, 147–170, 1979.
- Lapointe, B. E., Barile, P. J., Littler, M. M., and Littler, D. S.: Macroalgal blooms on southeast Florida coral reefs: II. Cross-shelf discrimination of nitrogen sources indicates widespread assimilation of sewage nitrogen, Harmful Algae, 4, 1106–1122, 2005.
- Lehmann, M. F., Sigman, D. M., and Berelson, W. M.: Coupling the $^{15}\text{N}/^{14}\text{N}$ and $^{18}\text{O}/^{16}\text{O}$ of nitrate as a constraint on benthic nitrogen cycling, Mar. Chem., 88, 1–20, 2004.
- Lévêque, C.: River and stream ecosystems of northwestern Africa, in: River and Stream Ecosystems, edited by: Cushing, C. E., Cummins, K. W., and Minshall, G. W., Elsevier Science B. V., Amsterdam, 519–536, 1995.
- Marion, G. S., Dunbar, R. B., Mucciarone, D. A., Kremer, J. N., Lansing, J. S., and Arthawiguna, A.: Coral skeletal $\delta^{15}\text{N}$ reveals isotopic traces of an agricultural revolution, Mar. Pollut. Bull., 50, 931–944, 2005.
- Mayorga, E., Seitzinger, S. P., Harrison, J. A., Dumont, E., Beusen, A. H. W., Bouwman, A. F., Fekete, B. M., Kroeze, C., and Van Drecht, A.: Global nutrient export from WaterSheds 2 (NEWS 2): model development and implementation, Environ. Modell. Softw., 25, 837–853, 2010.
- McGuire, K. and McDonnell, J.: Stable isotope tracers in watershed hydrology, in: Stable isotopes in ecology and environmental science, 2nd edited by: Michener, R. and Lajtha, K., Blackwell Publishers, Boston, Massachusetts, 334–374, 2007.
- Mengis, M., Gachter, R., and Wehrli, B.: Sources and sinks of nitrous oxide (N_2O) in deep lakes, Biogeochemistry, 38, 281–301, doi:10.1023/A:1005814020322, 1997.
- Mogaka, H., Gichere, S., Davis, R., and Hirji, R.: Climate variability and water resources degradation in Kenya: improving water resources development and management, World Bank Working Papers, 69, 2006.
- Mook, W. G. and De Vries, J. J.: Environmental isotopes in the hydrological cycle: principles and applications, Vol. 3, Surface Water, 2000.
- Moynihan, M. A., Baker, D. M., and Mmochi, A. J.: Isotopic and microbial indicators of sewage pollution from Stone Town, Zanzibar, Tanzania, Mar. Pollut. Bull., 64, 1348–1355, 2012.
- Mutisya, D. K. and Tole, M.: The impact of irrigated agriculture on water quality of rivers Kongoni and Sirimon, Ewaso Ng'iro North Basin, Kenya, Water Air Soil Poll., 213, 145–149, 2010.
- Ohowa, B. O.: Seasonal variations of the nutrient fluxes into the Indian Ocean from the Sabaki river, Kenya, Discov. Innovat., 8, 265–274, 1996.
- Olima, W.: Dynamics and implications of sustaining urban spatial segregation in Kenya – experiences from Nairobi metropolis, in: International Seminar on Segregation in the City, Lincoln Institute of Land Policy, Cambridge, USA, World Health Organization (WHO), 2001.
- Ongwenyi, G. S., Kithiia, S. M., and Denga, F. O.: An overview of the soil erosion and sedimentation problems in Kenya, IAHS Press, Wallingford, United Kingdom, 1993.
- Oosterom, A. P.: The geomorphology of southeast Kenya, Ph.D. thesis, Agricultural University, Wageningen, the Netherlands, 1988.
- Owens, N. J. P.: Natural variations in ^{15}N in the marine environment, Adv. Mar. Biol., 24, 390–451, 1987.
- Rajkumar, A. N., Barnes, J., Ramesh, R., Purvaja, R., and Upstill-Goddard, R.: Methane and nitrous oxide fluxes in the polluted Adyar River and estuary, SE India, Mar. Pollut. Bull., 56, 2043–2051, doi:10.1016/j.marpolbul.2008.08.005, 2008.
- Ravishankara, A. R., Daniel, J. S., and Portmann, R. W.: Nitrous oxide (N_2O): the dominant ozone-depleting substance emitted in the 21st century, Science, 326, 123–125, 2009.
- Richey, J. E., Devol, A. H., Wofsy, S. C., Victoria, R., and Riberio, M. N. G.: Biogenic gases and the oxidation and reduction of carbon in Amazon River and floodplain waters, Limnol. Oceanogr., 33, 551–561, 1988.
- Risk, M. J., Sayer, B. G., Tevesz, M. J., and Karr, C. D.: Comparison of the organic matrix of fossil and recent bivalve shells, Lethaia, 29, 197–202, 1997.
- Risk, M. J., Lapointe, B. E., Sherwood, O. A., and Bedford, B. J.: The use of $\delta^{15}\text{N}$ in assessing sewage stress on coral reefs, Mar. Pollut. Bull., 58, 793–802, 2009.
- Sebilo, M., Billen, G., Grably, M., and Mariotti, A.: Isotopic composition of nitrate-nitrogen as a marker of riparian and benthic denitrification at the scale of the whole Seine River system, Biogeochemistry, 63, 35–51, 2003.
- Sebilo, M., Billen, G., Mayer, B., Billiou, D., Grably, M., Garnier, J., and Mariotti, A.: Assessing nitrification and denitrification in the Seine River and estuary using chemical and isotopic techniques, Ecosystems, 9, 564–577, 2006.
- Seitzinger, S. P. and Kroeze, C.: Global distribution of nitrous oxide production and N inputs in freshwater and coastal marine ecosystems, Global Biogeochem. Cy., 12, 93–113, 1998.
- Seitzinger, S. P., Mayorga, E., Bouwman, A. F., Kroeze, C., Beusen, A. H. W., Billen, G., Van Drecht, G., Dumont, E., Fekete, B. M., Garnier, J., and Harrison, J. A.: Global river nutrient export: a scenario analysis of past and future trends, Global Biogeochem. Cy., 24, GB0A08, doi:10.1029/2009GB003587, 2010.
- Sherwood, O. A., Scott, D. B., Risk, M. J., and Guilderson, T. P.: Radiocarbon evidence for annual growth rings in the deep-sea octocoral *Primnoa resedaeformis*, Mar. Ecol.-Prog. Ser., 301, 129–134, 2005.

- Tamooh, F., Van den Meersche, K., Meysman, F., Marwick, T. R., Borges, A. V., Merckx, R., Dehairs, F., Schmidt, S., Nyunja, J., and Bouillon, S.: Distribution and origin of suspended matter and organic carbon pools in the Tana River Basin, Kenya, *Biogeosciences*, 9, 2905–2920, doi:10.5194/bg-9-2905-2012, 2012.
- Taylor, P. G. and Townsend, A. R.: Stoichiometric control of organic carbon–nitrate relationships from soils to the sea, *Nature*, 464, 1178–1181, 2010.
- Thomas, H., Schiettecatte, L.-S., Suykens, K., Koné, Y. J. M., Shadwick, E. H., Prowe, A. E. F., Bozec, Y., de Baar, H. J. W., and Borges, A. V.: Enhanced ocean carbon storage from anaerobic alkalinity generation in coastal sediments, *Biogeosciences*, 6, 267–274, doi:10.5194/bg-6-267-2009, 2009.
- Tiffen, M., Mortimore, M., and Gichuki, F.: More people less erosion: environmental recovery in Kenya, ACTS Press, Nairobi, Kenya, 33–43, 1994.
- Townsend, S. A., Webster, I. T., and Schult, J. H.: Metabolism in a groundwater-fed river system in the Australian wet/dry tropics: tight coupling of photosynthesis and respiration, *J. N. Am. Benthol. Soc.*, 30, 603–620, 2011.
- Trimmer, M., Grey, J., Heppell, C. M., Hildrew, A. G., Lansdown, K., Stahl, H., and Yvon-Durocher, G.: River bed carbon and nitrogen cycling: state of play and some new directions, *Sci. Total Environ.*, 434, 143–158, 2012.
- Van Katwijk, M., Meier, N. F., Loon, R. V., Hove, E. V., Giesen, W. B. J. T., Velde, G. V. D., and Hartog, C. D.: Sabaki river sediment load and coral stress: correlation between sediments and condition of the Malindi-Watamu reefs in Kenya (Indian Ocean), *Mar. Biol.*, 117, 675–683, 1993.
- Vitoria, L., Otero, N., Soler, A., and Canals, A.: Fertilizer characterization: isotopic data (N, S, O, C, and Sr), *Environ. Sci. Technol.*, 38, 3254–3262, 2004.
- Vitousek, P. M., Aber, J. D., Howarth, R. W., Likens, G. E., Matson, P. A., Schindler, D. W., Schlesinger, W. H., and Tilman, D. G.: Human alteration of the global nitrogen cycle: sources and consequences, *Ecol. Appl.*, 7, 737–750, 1997.
- Weiner, S., Lowenstam, H. A., Taborek, B., and Hood, L.: Fossil mollusk shell organic matrix components preserved for 80 million years, *Paleobiology*, 5, 144–150, 1979.
- Weiss, R. F.: Determinations of carbon dioxide and methane by dual catalyst flame ionization chromatography and nitrous oxide by electron capture chromatography, *J. Chromatogr. Sci.*, 19, 611–616, 1981.
- Weiss, R. F. and Price, B. A.: Nitrous oxide solubility in water and seawater, *Mar. Chem.*, 8, 347–359, 1980.
- Wetzel, R. G.: *Limnology*, 3rd Edn., Lake and river ecosystems, Academic Press, San Diego, 2001.
- Widory, D., Petelet-Giraud, E., Negrel, P., and Ladouche, B.: Tracking the sources of nitrate in groundwater using coupled nitrogen and boron isotopes: a synthesis, *Environ. Sci. Technol.*, 39, 539–548, 2005.
- Wrage, N., Velthof, G. L., van Beusichem, M. L., and Oenema, O.: Role of nitrifier denitrification in the production of nitrous oxide, *Soil Biol. Biochem.*, 33, 1723–1732, doi:10.1016/S0038-0717(01)00096-7, 2001.
- Yamamoto, S., Alcauskas, J. B., and Crozier, T. E.: Solubility of methane in distilled water and seawater, *J. Chem. Eng. Data*, 21, 78–80, 1976.
- Yasin, J. A., Kroeze, C., and Mayorga, E.: Nutrients export by rivers to the coastal waters of Africa: past and future trends, *Global Biogeochem. Cy.*, 24, GB0A07, doi:10.1029/2009GB003568, 2010.
- Zhang, G.-L., Zhang, J., Liu, S.-M., Ren, J.-L., and Zhao, Y.-C.: Nitrous oxide in the Changjiang (Yangtze River) Estuary and its adjacent marine area: Riverine input, sediment release and atmospheric fluxes, *Biogeosciences*, 7, 3505–3516, doi:10.5194/bg-7-3505-2010, 2010.
- Zurbrugg, R., Suter, S., Lehmann, M. F., Wehrli, B., and Senn, D. B.: Organic carbon and nitrogen export from a tropical dam-impacted floodplain system, *Biogeosciences*, 10, 23–38, doi:10.5194/bg-10-23-2013, 2013.